

Chapter 17

Recent Advances in Direct-Drive Power Take-Off (DDPTO) Systems for Wave Energy Converters Based on Switched Reluctance Machines (SRM)



Marcos Blanco, Jorge Torres, Miguel Santos-Herrán, Luis García-Tabarés, Gustavo Navarro, Jorge Nájera, Dionisio Ramírez, and Marcos Lafoz

Abstract This chapter is focused on Power Take-Off (PTO) systems for wave energy converters (WEC), being one of the most important elements since PTOs are responsible to transform the mechanical power captured from the waves into electricity. It presents Direct-Drive PTO (DDPTO) as one of the most reliable solutions to be adapted to some particular types of WEC, such as point absorbers. A discussion about modularity and adaptability, together with intrinsic characteristics of direct-drive PTOs, is also included. Among the different technologies of electric machines that can be used in direct-drive linear PTOs, switched reluctance machines (SRM) are described in further detail. In particular, the Azimuthal Multi-translator SRM is presented as a suitable solution in order to increase power density and reduce costs. Not only the electric machine, but also the associated power electronics are described in detail. The description includes the different configurations and topologies of power converters and the most appropriate control strategies. Finally, a superconducting linear generator solution is described, presenting it as a reliable alternative for the application of direct-drive PTOs. An example of concept and preliminary

M. Blanco · J. Torres · M. Santos-Herrán (✉) · L. García-Tabarés · G. Navarro · J. Nájera · M. Lafoz
CIEMAT, Avda. Complutense 40, 28045 Madrid, Spain
e-mail: miguel.santos@ciemat.es

M. Blanco
e-mail: marcos.blanco@ciemat.es; marcos.blanco.aguado@ciemat.es

J. Torres
e-mail: jorgejesus.torres@ciemat.es

J. Nájera
e-mail: jorge.najera@ciemat.es

M. Lafoz
e-mail: marcos.lafoz@ciemat.es

D. Ramírez
ETSII-UPM, Cale José Gutiérrez Abascal 2, 28006 Madrid, Spain
e-mail: Dionisio.ramirez@upm.es

design is included in order to highlight the main challenges to be faced during this process.

17.1 Introduction

The Power Take-Off (PTO) system is the Wave Energy Converter (WEC), which is the component in charge of extracting the energy from the ocean resource. It is a key element at the core of the energy conversion process from the ocean waves to a final usable form of energy, e.g. electricity. From an economical perspective, it is forecasted that PTOs are going to become one of the main contributors to the wave energy arrays cost [1], representing up to 20–22% of the lifetime costs [2–4].

Accordingly, PTOs have always been at the focus of the research, development, and innovation in the wave energy sector. For instance, the Joint Research Centre (JRC), i.e. the science and knowledge service of European Commission (EC), has identified PTOs as one of the key technological priorities for wave energy since 2014 [5, 6]. In fact, the Strategic Research and Innovation Agenda (SRIA) for Ocean Energy developed under the project ETIP Ocean, which was released in 2020, still recognises “*improvement and demonstration of PTO and control systems*” as a challenge area and a priority topic for the design and validation of ocean energy devices [7]. Moreover, it is crucial for allowing ocean energy to become an essential contributor to the upcoming European Green Deal. As a consequence, in the recent years, EC has funded several projects addressing the development and optimisation of PTOs for wave energy conversion under the Horizon 2020 calls, such as OPERA, WaveBoost, WETFEET, IMAGINE and SEA-TITAN.¹

The significance of PTO development as one of the key actions for an adequate progress in the sector was reinforced in 2015 with the creation of the Power Take-Off funding programme by Wave Energy Scotland (WES). To date, WES has supported 17 different projects under this PTO-specific call, providing GBP 17.5 million of funding. Furthermore, in 2018 the JRC held a workshop on the identification of future emerging technologies in the ocean energy sector [8], where innovative PTOs were found to be one of the nine main emerging technology families.

Given the aforementioned weight of the PTO cost shared in the total project costs, any potential cost reduction in this component might result in important savings in the final Levelised Cost of Energy (LCOE). This is especially relevant due to the current needs for cost reduction in the wave energy sector to foster its entry into the market. The Carbon Trust estimated that technical advances on PTOs for wave energy applications would lead to a cost centre progress rate of 93% [9], i.e. for each doubling of the installed capacity, a 7% reduction in PTO cost is achieved. For its part, WES identified PTO performance (in terms of conversion efficiency) and PTO reliability (in terms of availability) as the most relevant characteristics to drive potential LCOE cost reductions [10]. In this sense, a sensitivity analysis applied to

¹ Project Information can be consulted in <https://cordis.europa.eu/project/>.

a representative example found that a 10% improvement in efficiency or reliability could generate savings of 9% in the total LCOE. Similar results were found by the Partnership for Wave Energy in Denmark [11].

17.2 Power Take-Off (PTO) in Wave Energy Converters

17.2.1 Introduction to PTO-Concept

In 2007, the International Electrotechnical Commission (a worldwide standardisation organisation) established a Technical Committee dedicated to marine energy: TC114. Given the rapid growth of the emerging wave, tidal and water current energy industry, it became necessary to develop a Technical Specification (TS) presenting a common basis for language and nomenclature in the sector. *IEC TS 62600-1 Marine energy—Wave, tidal and other water current converters: Terminology* was released in 2011 (and amended in 2019). According to this TS, a PTO is defined as the “*mechanism that converts the motion of the prime mover into a useful form of energy such as electricity*”, where “*prime mover*” is the “*physical component that acts as the interface between the marine resource and the energy converter from which energy is captured [Note 1 to entry: For wave energy converters the prime mover may be a heaving buoy, a hinged flap, an OWC runner, etc.]*”.

It must be highlighted that the motion experienced by the prime mover will be determined not only by the excitation from the marine energy resource (i.e. the waves), but also by the characteristics of the PTO, which is able to create force/torque acting on the former. The main advantage of this force/torque lies in its controllability. Thus, the PTO can be considered equivalent to the “brain” of the WEC, since it is able to impose the necessary dynamics so that the prime mover-wave interaction maximises the energy extraction. This can only be achieved by means of a control system, which is responsible for adapting the WEC to a desirable behaviour under different load conditions (i.e. maximising energy generation during operation times; minimising the risk to the device in survivability mode; etc.).

17.2.2 Introduction to the Different Types of PTOs

As opposed to wind energy technology, or even tidal, where designs have focused on horizontal-axis machines, there is a lack of industrial convergence towards a common design or device in wave energy conversion. The European Marine Energy Centre (EMEC) in Scotland (UK) offers a comprehensive compilation of wave energy developers in the world. According to the latest update (in August 2020) [12], the most numerous device family—point absorbers—represents only 83 of the total 255 known devices, i.e. one third. Other relevant WEC families include attenuators,

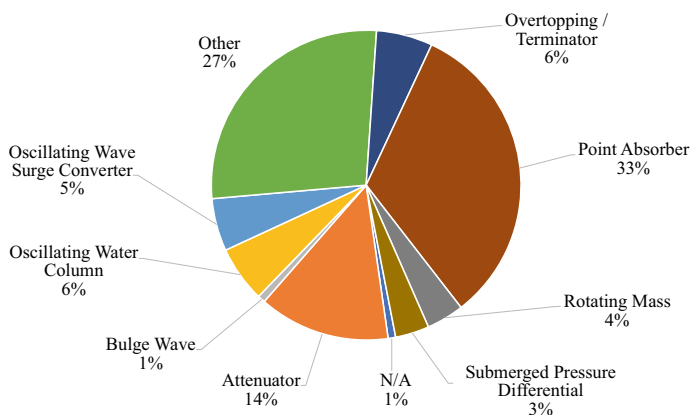


Fig. 17.1 Distribution of wave energy technologies according to EMEC's WEC-classification [12]

overtopping/terminators, oscillating water columns (OWC), or oscillating wave surge converters, as it can be observed in Fig. 17.1.

Wave energy PTOs are not oblivious to this technology diversity, and the aforementioned heterogeneity is transferred to their designs. Several PTO concepts have been investigated to date, given the existing connection between WEC and PTO typologies. For instance, on the one hand, OWCs will highly likely incorporate air turbines as their PTO, since their working principle consists of an oscillation in air pressure inside a chamber caused by the ocean waves. On the other hand, hydraulic PTOs will be probably utilised in WECs experiencing motions caused by high forces at low frequencies (e.g. attenuators or oscillating wave surge converters).

PTOs can be classified according to the type of energy conversion(s) in the path from ocean waves to electricity (see Fig. 17.2). Usually, the energy absorbed by the prime mover is firstly transformed into an intermediate form of energy, able to drive a rotary generator at which, secondly, this mechanical energy is converted into electricity. However, some PTO concepts, such as direct electrical drives or dielectric elastomers, can reduce this energy conversion process to a single step.

The vast majority of PTOs in wave energy conversion are dedicated to the generation of electricity. However, in some cases, the output is the production of pressurised water for desalination purposes (as proposed, for example, by Aquamarine Power with their Oyster device or by Carnegie Wave) [13]. Examples of the integration of PTOs, from the different families presented in Fig. 17.1, into wave energy converters can be seen in Fig. 17.3.

The main challenge for PTOs is the adaptation of the irregular high-power low-velocity wave energy resource to an acceptable form of electricity for the grid. Direct drive solutions are systems that directly couple the mechanical energy of the prime mover to the moving part of an electrical generator (the 'rotor' in rotary machines or 'translator' in linear ones). The coupling can be achieved either via a mechanical transmission system and gearbox (*direct mechanical drive systems*) or without

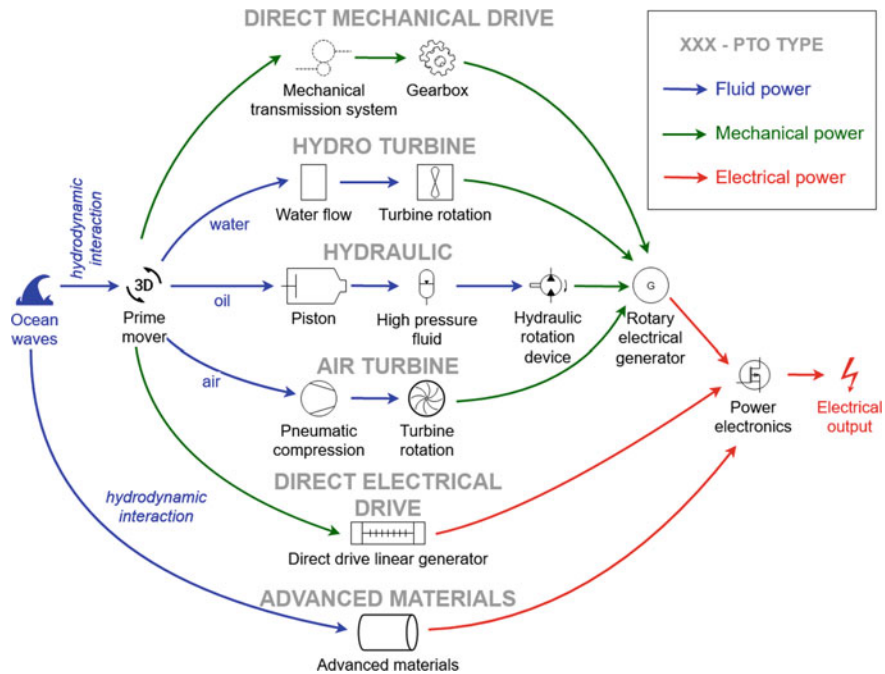


Fig. 17.2 Alternatives for wave energy to electricity conversion. Adapted from Magagna and Uihlein [6] and Têtu [11]

it (*direct electrical drive systems*). The benefit of employing direct drive systems lies in the removal of intermediate energy conversion stages, hence eliminating common failure sources (e.g. hydraulic components) and increasing its efficiency and reliability.

In the past, hydraulic systems used to represent the most common PTO type in wave energy conversion, accounting for around 40% of the total share in 2014 [6]. Nevertheless, in the recent years, the sector has witnessed an increased interest in direct-drive PTOs, moving from a 30% total PTO share representation in 2014 [6] to more than 40% in 2020 [19]. From the total of 98 active wave energy technology developers identified in [19], 31 companies are using direct mechanical drive systems, whereas in 13 cases direct electrical drives are considered.

Examples of real-sea deployments of WECs based on direct drive PTO systems and their characteristics [19–21] are listed in Table 17.1 (direct mechanical drive) and In the case of direct electrical drive systems, the absence of gearboxes allows to reduce noise levels and simplify drive train configurations [24], while the lower maintenance requirements led to increased availability and reduced lifetime costs. Furthermore, direct electrical drive machines increase the overall controllability of the WEC, since modern power electronics and control systems highly improve the performance of all electrical machines. This feature is of special relevance because it permits to implement more efficient strategies that maximise the energy harvesting

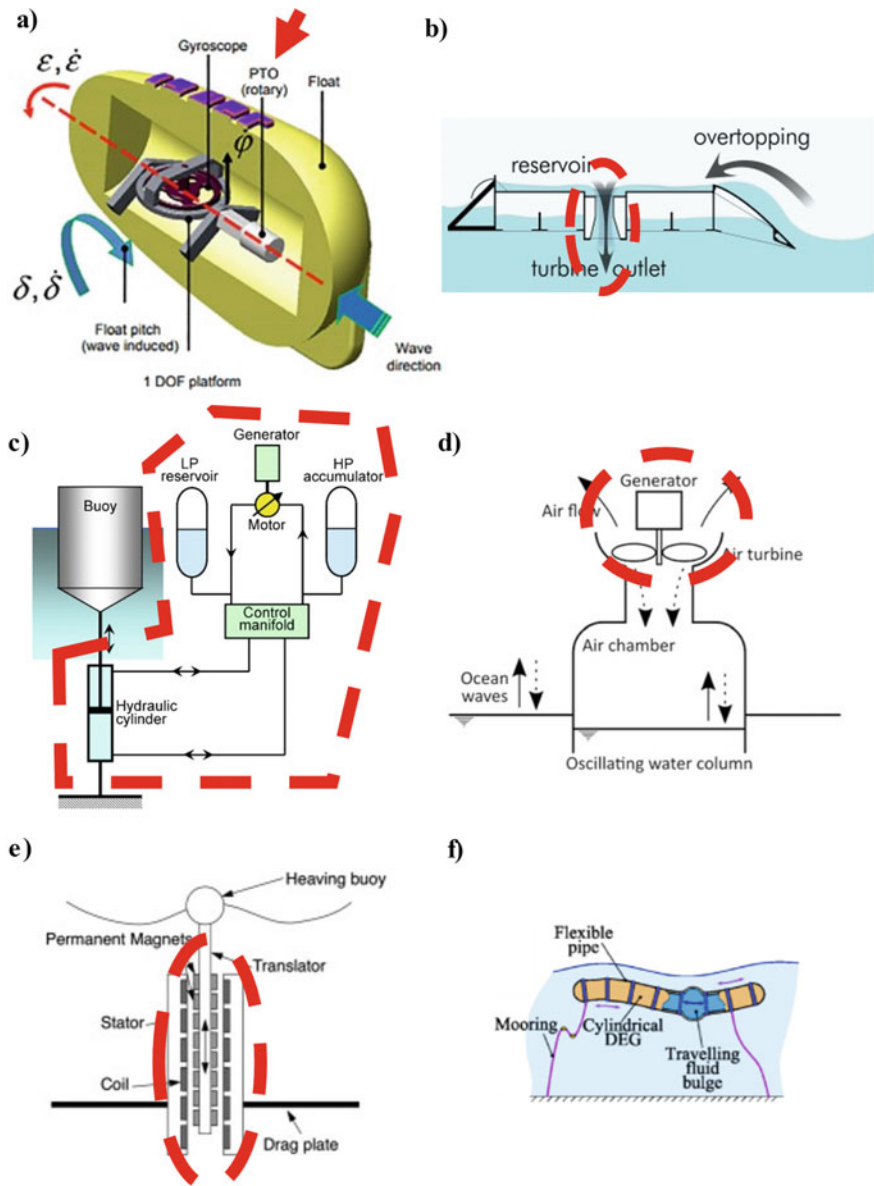


Fig. 17.3 Examples of PTO integration: **a** direct mechanical drive (taken from Liu et al. [14]); **b** hydro turbine (taken from [15]); **c** hydraulic (taken from Falcão [16]); **d** air turbine (taken from Têtu [11]); **e** direct electrical drive (taken from Drew et al. [17]); **f** advanced materials (taken from Moretti et al. [18]). The PTO components are indicated in red (Note that in the last case, the PTO and the prime mover are coincident, since the whole bulge-wave WEC is made of dielectric elastomer generators [DEGs])

Table 17.1 Direct mechanical drive PTO based WECs

WEC name	Technology developer	Website/references	Country of deployment	Year of deployment	Features	Rated power (kW)
Penguin	Wello	https://wello.eu/ [22]	UK	2012, 2017	Off-centre mass gyration drives a spinning flywheel	1000
Smart Power Buoy	Resen Waves	http://www.resenwaves.com/	Denmark	2017	Gearbox	0.6
C3	CorPower	https://www.corpowerocean.com/	UK	2018	Mechanical transmission by Cascade gearbox	25
EMERGE WEC	UmbraGroup	https://www.umbraagroup.com/ [23]	UK	2019	Integration of a recirculating ballscrew and a permanent magnet generator	200
LAMWEC	Laminaria	http://www.laminaria.be/	UK	2020–2021	Drum pulley system	200

from the ocean wave resource. Therefore, the PTO concept cannot be limited to the electrical generator and must include the associated power electronics and control system. On the other hand, the main disadvantage of direct drives systems is that manages velocities—that are directly the velocities of the WEC prime mover—which are lower than conventional rotary generators equivalent speeds due to the low ocean waves frequencies. Consequently, the required forces are bigger. Since the force grows linearly with the current while the losses increase as the square of the current, these high force machines tend to be less efficient. These high forces give rise to very large machines and a heavy/robust structures due to the attractive forces between the stator and the translator [25].

Table 17.2 (direct electrical drive).

In the case of direct electrical drive systems, the absence of gearboxes allows to reduce noise levels and simplify drive train configurations [24], while the lower maintenance requirements led to increased availability and reduced lifetime costs. Furthermore, direct electrical drive machines increase the overall controllability of the WEC, since modern power electronics and control systems highly improve the performance of all electrical machines. This feature is of special relevance because it permits to implement more efficient strategies that maximise the energy harvesting

Table 17.2 Direct electrical drive PTO based WECs

WEC name	Technology developer	Website	Country of deployment	Year of deployment	Features	Rated power
AWS I	AWS Ocean Energy	http://www.awsocan.com/ [16]	Portugal	2004	Permanent-magnet linear synchronous generator	2000 kW
Wavebob	Wavebob	N/A [26]	Ireland		Linear electric generator	
L10	Oregon State University	https://oregonstate.edu/ [27]	USA	2008	Permanent-magnet tubular linear generator	10 kW
W1	Wedge Global	https://wedglobal.com/ [28]	Spain	2014	Switched Reluctance Machine	200 kW
SP WEC	SINN Power	https://www.sinnpower.com/ [13]	Greece	2015–2019		18 and 36 kW
Seabased	Seabased	https://seabased.com/ [22]	Sweden	2015	Longitudinal flux permanent magnet generator	30 kW
C-GEN Neptune	University of Edinburgh	https://www.cgen.eng.ed.ac.uk/ [29]	UK	2019	Transverse flux permanent magnet	150 kW
StingRAY H2	Columbia Power Technologies	https://cpower.co/ [30]	USA	2020–2021	LandRAY: rotary permanent magnet generator	500 kW

from the ocean wave resource. Therefore, the PTO concept cannot be limited to the electrical generator and must include the associated power electronics and control system. On the other hand, the main disadvantage of direct drives systems is that manages velocities—that are directly the velocities of the WEC prime mover—which are lower than conventional rotary generators equivalent speeds due to the low ocean waves frequencies. Consequently, the required forces are bigger. Since the force grows linearly with the current while the losses increase as the square of the current, these high force machines tend to be less efficient. These high forces give rise to very large machines and a heavy/robust structures due to the attractive forces between the stator and the translator [25].

The following section in this chapter will focus on the aforementioned direct electrical drive systems, hereinafter directly referred to as Direct-Drive Power Take-Offs (DDPTO).

17.3 Direct-Drive Power Take-Off: SRM Topology

17.3.1 *Introductory Aspects*

DDPTOs are very attractive due to the improvement in the overall efficiency and in the controllability of a WEC. In fact, they make possible the implementation of more efficient energy extraction strategies, but with the force capability limitation of the DDPTO. Since the velocity of the motions involved in WECs is small, 1 m/s as order of magnitude, the forces required to achieve typical renewable-energy power values are several orders of magnitude higher; e.g. a device which is designed to harvest 1 MW of energy, needs to produce a force in the order of MN.

From a comparative point of view, conventional rotating machines are very common to be found working in this range of power but at much higher velocity and much lower torques. Therefore, the best option to increase the relative velocity between the moving parts of the WEC is the combination of a DDPTO and a WEC working close to resonance, since the same power can be extracted from the waves with significantly less force than what is needed when operating far from resonance.

High power generators are long and heavy. The relatively high moving velocity which are involved limit the minimum airgap between both sides leading to stiff designs with strict tolerances. As explained before, big forces require big currents and consequently higher Joule losses, which will be associated to additional heat dissipation. Thermal calculations and design also become more relevant.

Therefore, all these points make a discussion about an attractive alternative (not exclusive) for increasing the force density of the PTO consisting of using superconducting coils. For the same level of machine power, the superconducting machine can be a solution to reduce size and weight (see Sect. 17.4). Excluding the superconducting machine, there are three possible main candidates of electric machines for using in a Power Take-Off (PTO) considering their operation principle. These three alternatives will be discussed in Sect. 17.3.3 [31, 32].

- Permanent Magnet Machines (PMM), including Permanent Magnet Synchronous Machines (PMSM)
- Variable Reluctance Machines (VRM), including Synchronous or Switched Reluctance Machines (SRM)
- Special machines based on a combination of the previous ones, like Vernier Machines or other Transverse Flux Permanent Magnet Machines.

One important issue in the linear electrical generators is the configuration of the machine, especially which part of the machine is the longer and the shorter one, since it affects to the size and weight of the system. Figure 17.4a shows an example of a linear machine configuration that balances transverse forces, in which all the developed DDPTOs are based on. In this case, the length of the stator (m) is smaller than the length of the translator (m) by twice the stroke of the PTO (s) [28, 33, 34]. Mechanical and electromagnetic considerations allow defining the geometrical requirements for the linear electrical machine to be used in the PTO:

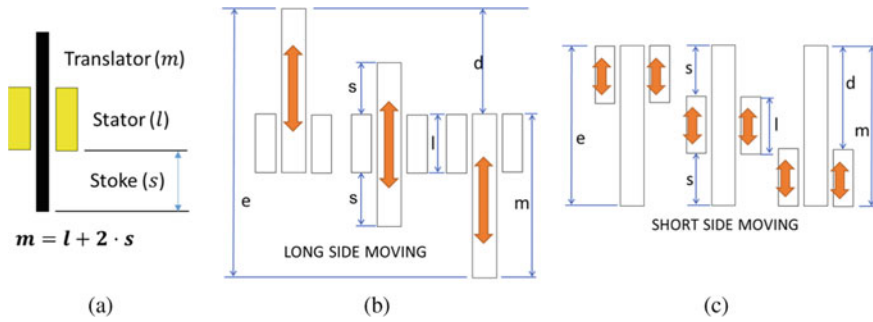


Fig. 17.4 **a** Example of short stator configuration; **b** Long side moving; **c** Short side moving

- *Stroke (s)*: This parameter is basically defined by its localization, the wave height and the operation mode (resonant or not). Even for small waves, the maximum amplitude of the translator motion (stroke) can be high if the point absorber works close to resonance. Combination of high waves and resonance usually lead to inadmissible values for the stroke, which must be limited.
- *Stator and Translator Dimensions*: The geometrical parameter constrains are defined based on the concept of Shear Stress (σ), which is the force that any electrical machine is able to produce by unit surface of its airgap. This variable is very useful in the analysis of an electrical machine for a PTO. The value of σ is proportional to the product of the electric load of the machine (expressed in kA/m) times the magnetic load of the machine (expressed in Tesla).

E.g. a typical value for PMSM spans from 20 to 40 kN/m² according to the magnetic flux density in the airgap (1–1.3 T) and the electric load (20–50 kA/m), which depends on the windings current density and their cooling system [24].

Based on that, each of the two sides on the machine can be classified according to four parameters:

- Its role: Which part of the machine is the active one and which is the passive one. The active part is where the coils are placed, and the passive one is the part which closes the magnetic circuit but does not include any coil that delivers active power to the system (e.g. in VRM, the part which only contains the magnetic steel; in PMSM, the part which includes the permanent magnets; in a conventional a synchronous machine, the part where the excitation coils are placed).
- Its length: Based on this parameter, there are two possibilities: to be a long or a short part. Making an analogy with a rotary machine, the ‘short’ part would represent 360 electrical degrees of it, therefore it would mean to a ‘unit module’ of the machine. On the other hand, the ‘long’ part is an integer multiple of the unit module, i.e. the overlapped part with the ‘short’ one. The difference between the length of the ‘long’ and the ‘short’ part is the total stroke of the linear machine.
- Its position: It could be external or internal. The part which surrounds the other one, is considered as external.

Table 17.3 Machine design parameters according to the configuration

	Long side moving	Short side moving
Stroke (<i>s</i>)	According to the PTO	According to the PTO
Short-side length (<i>l</i>)	According to the force	According to the force
Long-side length (<i>m</i>)	$m = l + s$	$m = l + s$
Displacement (<i>d</i>)	$d = s$	$d = s$
Machine envelope (<i>e</i>)	$e = 2 \cdot s + l$	$e = s + l$

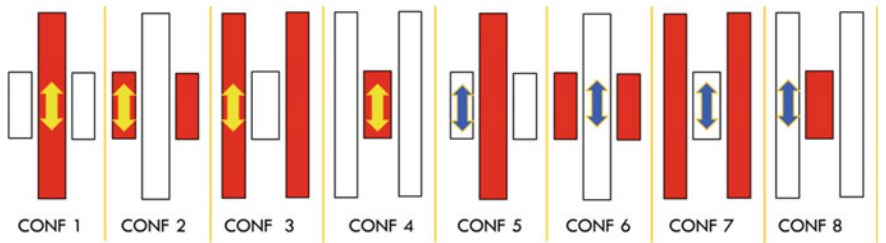


Fig. 17.5 Geometrical configurations of DDPTO. Active side (AS) in red | Passive side (PS) in white

- Its velocity: They could be defined as moving part or stationary part.

According to these parameters, there are different possible configurations. Figure 17.4b, c show two configurations, depending on whether the short part is moving or fixed, and for those possibilities, Table 17.3 shows the size of each part. The short-side length “*l*” is the length of the active side and depends on the rated generated force. Due to the linear machine envelope “*e*” is the length required by the structure to host the whole machine, it can be remarked that the power density for a generator with external translator is higher than for a generator with an internal one [35]. Based on this, Fig. 17.5 shows the possible configurations considering both possibilities (short or long moving) and the roles (active or passive). Additionally, a table with advantages and drawbacks for each alternative is included (Table 17.4).

17.3.2 Example of an Analysis of a WEC with a DDPTO

In this section, an example of a WEC with a linear electrical generator is analysed in order to show the impact of the DDPTO characteristics (efficiency, rated force, etc.) in the overall WEC energy extraction capacity. This study illustrates the need of a high-force PTO applied to a particular example, the Heaving Point-Absorber

Table 17.4 Advantages and drawbacks of the linear generator (DDPTO) geometrical configuration

CONF.	Geometrical Conf.	Advantages and drawbacks
CONF 1	AS: Long, Int. & Moving PS: Short, Ext. & Stationary	UNFEASIBLE <u>Cons.</u> : long and moving active side
CONF 2	AS: Short, Ext. & Moving PS: Long, Int. & Stationary	NOT PREFERABLE <u>Cons.</u> : The movement transmission is external and required flexible electrical connections
CONF 3	AS: Long, Ext. & Moving PS: Short, Int. & Stationary	UNFEASIBLE <u>Cons.</u> : Similar to CONF 1 but even worse since the movement transmission must be external
CONF 4	AS: Short, Int. & Moving PS: Long, Ext. & Stationary	FEASIBLE <u>Cons.</u> : Moving the active part and required flexible electrical connections/ <u>Adv.</u> : The moving mass can be small, the passive side can be part of the structure and the spar shorter
CONF 5	AS: Long, Int. & Stationary PS: Short, Ext. & Moving	NOT PREFERABLE <u>Cons.</u> : The active side must be long and the movement transmission must be external
CONF 6	AS: Short, Ext. & Stationary PS: Long, Int. & Moving	FEASIBLE <u>Cons.</u> : The stroke is long, and the PS weight could be excessive <u>Adv.</u> : Simplest configuration
CONF 7	AS: Long, Ext. & Stationary PS: Short, Int. & Moving	NOT PREFERABLE <u>Adv.</u> : It could be considered for short strokes and high forces, where the length of the AS is not much smaller than the overall length
CONF 8	AS: Short, Int. & Stationary PS: Long, Ext. & Moving	NOT PREFERABLE <u>Cons.</u> : Similar to CONFG 6 but the moving side can be even heavier, and the transmission must be external

(HPA) W1 prototype [36]. The results are obtained from a mathematical model, experimentally validated in the referred WEC (Fig. 17.6).

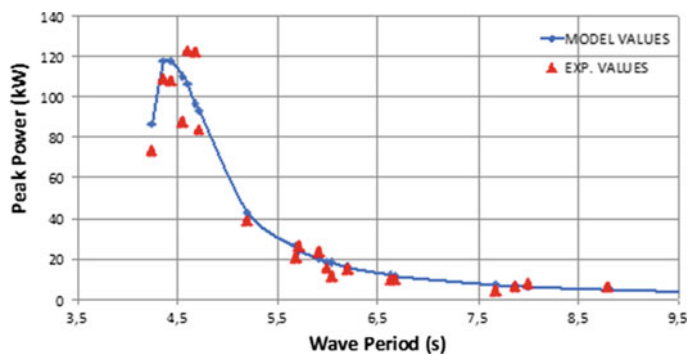


Fig. 17.6 Peak generated power predictions and measurements for the W1 WEC normalised to 1 m regular wave amplitude (fixed damping control strategy)

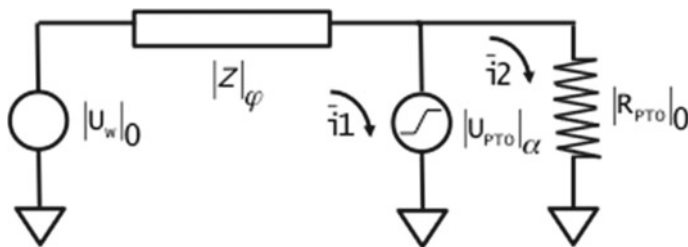


Fig. 17.7 Equivalent circuit of the PTO and WEC models [37, 38]

The model is based on the motion equations of two moving bodies of a HPA in the water, when they are excited by the presence of waves. The model is a simplified version where only the float movement is considered. Figure 17.7 shows the equivalent electrical circuit of this simplified model [37], including the following parameters:

- The two external forces acting on the HPA—wave excitation and PTO forces—are modelled with a voltage source U_w and U_{PTO}
- The float mechanical total impedance Z , which includes radiation, inertia (float mass plus added water mass) and buoyancy coefficients.
- The current equivalent to the velocities i_1 and i_2 .
- The PTO losses in the form of a parallel resistance R_{PTO} .

Firstly, a benchmark ideal case is calculated in order to compare with the real PTO. Therefore, these results for this base case are obtained using the previous model with a control strategy which maximizes the generated electrical power [39, 40] for regular waves, assuming an ideal PTO (100% of efficiency) with and without a maximum force limitation of 1 MN. These results are shown in Fig. 17.8a where the red curve shows the maximum power that can be extracted for each wave period, (i.e. ideal case where there are no limitations), while the orange one represents the power that

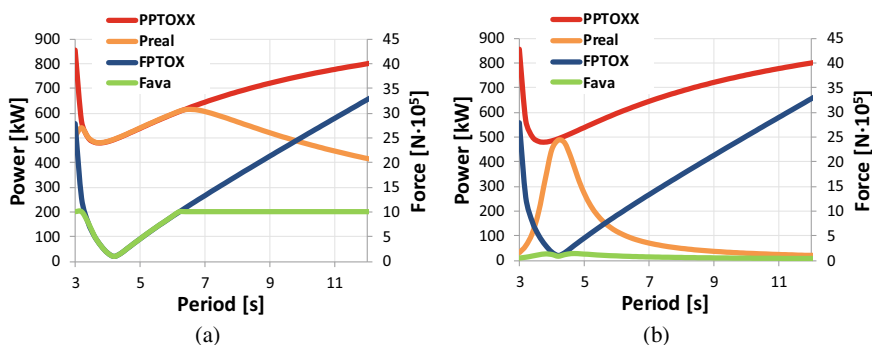


Fig. 17.8 Generated power and required force results obtained from the WEC & PTO models for different wave periods: **a** Ideal PTO; **b** Real PTO

is really extracted by a real PTO defined as benchmark. Moreover, Fig. 17.8a shows the required force to achieve the generated power for both cases, the PTO without limitations (blue curve) and the PTO with a limited force of 1 MN (green curve). Both curves orange and red one coincide in the range where the force is not limited, and as soon as the force limit acts, the orange curve is unable to follow the red one and the real extracted power starts to drop.

Next step is to consider a real PTO with losses (75% of efficiency). This parameter is estimated from the model developed during the experimental characterisation of the W1 prototype. These results are shown in Fig. 17.8b. The PTO has the same force limitation of 1 MN, nevertheless the results are totally different, since only in a narrow range of wave periods the PTO is able to extract the maximum available power. The rest of wave periods range, the extracted power by the real PTO (orange power) is smaller than the available power (red curve) and the force required by the PTO to extract that power (green curve) is well below the 1 MN limit. The reason is that the WEC control strategy prefers using less force than what is available to maximize energy production since losses for higher forces lead to a smaller energy production. Therefore, the main conclusion of the analysis is that the amount of energy which can be harvested from the waves in a wide range of periods for a real PTO with force restrictions and limited energy conversion efficiency drops dramatically with respect to what could be captured with an ideal lossless and force-unlimited PTO, as is shown in Fig. 17.9a.

Figure 17.9a shows an indicator to quantify the benefits of improving the PTO performance, especially the PTO force capability and efficiency. This parameter is quantified through the area enclosed by the electrical generated power curve, yellow area in the real PTO studied. This area will be named as Integrated Power Capture (IPC), expressed in kJ when power is expressed in kW. Moreover, the ratio between the IPC for a WEC with a real PTO and a WEC with an ideal one will be defined as the IPC Ratio (IPCR). The IPCR of a PTO could be improved augmenting the

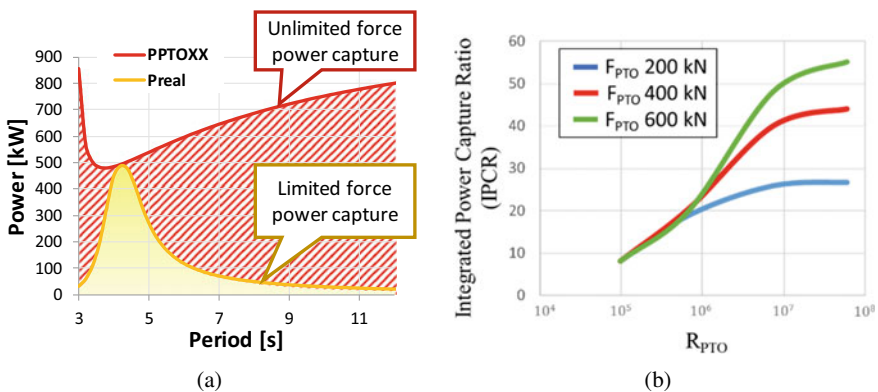


Fig. 17.9 **a** Integrated Power Capture Ratio (IPCR) concept; **b** IPCR versus PTO Resistance (R_{PTO}) for different PTO Forces (F_{PTO})

Force Capability, the Efficiency or both together. Figure 17.9b shows the effect of increasing the PTO force and efficiency, in terms of the parameter R_{PTO} , for the W1 PTO studied. In this study case, the dominant losses are the Joule losses, which are proportional to the square of the current and the force. The dependence of the R_{PTO} value in the IPCR is shown in Fig. 17.9b for three different force values (200, 400 and 600 kN), showing the mentioned benefits improving in the force level.

17.3.3 The Linear Switched Reluctance Machine (LSRM)

17.3.3.1 Introduction—Alternatives of Linear Electric Machines for Wave Energy Generation Application

Various types of linear electrical machines can be used for ocean wave energy conversion, as described in Sect. 17.3.1. The possible candidates for being used in a WEC are summarised in Fig. 17.10 and described in the following paragraphs [21].

Permanent Magnet Synchronous Machines (PMSM): The operating principle is based on the excitation from the magnets; the magnetic fields created move synchronously with the translator, at the same velocity, respect to the translator. As it occurs in other machines, force density could be increased using a double-sided configuration [41]. In this type of machines, two possible field configurations are used, longitudinal and transverse flux type. The implementation of a doubled-sided machine shows better performance than a single-sided machine according to the flux dispersion and bearing loads, since the lateral forces are fully compensated. One drawback of this type of machine is the cogging force produced by the interaction between rotor-stator magnetic fields. This effect reduces their efficiency in linear machines.

Lineal PM tubular machine: The operating principle of the PM tubular linear machine consists in the production of an electromotive force in a wire by means of changing the magnetic field (i.e. the force is generated by the interaction between the magnetic fields from the PMs and the currents on the coils). The translator must be perfectly aligned due to the fact that the force is perpendicular to the direction of the translator motion. The total cost of this type of linear machine is basically determined by the cost of the PM, usually Neodymium magnets due to their high

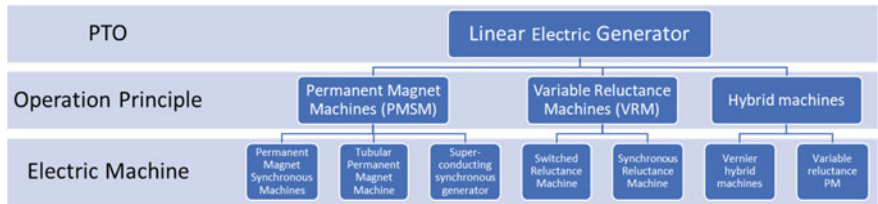


Fig. 17.10 Types of linear electric generators and assembly topologies for wave energy applications

magnetic field strength. Its main drawback is the de-magnetisation of the PMs after a certain time [42].

Linear superconducting synchronous machine: This topology has already been investigated for wind energy conversion. In such type of machine, superconducting magnets have been used instead of conventional ones in which a de-magnetisation effect appeared after a certain time. The typical wire used is the MgB2 [43], where its critical temperature is relatively high for the iron machines due to the fact that the magnetic field value is low.

- *Variable Reluctance Machines (VRM), including Switched Reluctance machines (SRM) and Synchronous Reluctance machines (SyRM) or:*

The operating principle of the linear SRM is similar to the rotating SRM and a stepper motor, it is based in the reluctance minimisation principle. The magnetic field is created from the stator current. The main advantages of these machines are their reliability, robustness, high efficiency and simple construction, lowest manufacturing cost due to the absence of magnets and high force. The operation of these machines is controlled by the translator position and a power electronic converter, similar to what occurs in a stepper motor. Due to its operating principle, its main drawback is the high force ripple compared to other topologies.

Regarding the SyRM, this topology has a similar structure as SRM since they have no permanent magnets mounted on their translators—based on salient poles—and the operating principle is the reluctance minimisation. Their stator structure is based on the induction machines, since the stator is wound with a distributed winding with 3 phases, which creates a rotating magnetic field in the air gap of the electric machine. This field rotates at synchronous speed and can be considered sinusoidal. The main drawback of this topology is its low power factor.

- *Vernier hybrid machines:*

Vernier hybrid machines are a type of variable reluctance machines. These machines offer a low power factor, but it can be improved by auxiliary DC field excitation winding [44]. In Vernier hybrid machines, magnets are placed on the stator to create the magnetomotive force and the translator is slotted, as occurs in a reluctance machine, to modulate the magnetic field [45, 46].

- *Variable reluctance PM (VRPM) machine:*

The operating principle of these machines is the reluctance force which comes out to be the same as that for DC machines, PMSM or field wound synchronous machines [47]. Variable reluctance machines can be assembled in transverse flux machines (TFMs) or in longitudinal flux machines (LFMs), presenting TFMs better performance than LFMs for ocean wave applications [48–50].

Once the description of all different types of linear machines for PTOs is finished, we present the main differences, in order to select the best configuration:

- The PMSMs needs a high number of permanent magnets to produce the field. Modern rare-earth magnets allow generating magnetic fields up to 1.3 T with

masses in the order of 75 kg/m^2 of machine airgap [51]. In summary, a 500 kN permanent magnet machine would require between 12.5 and 25 m^2 of active air gap surface and between 950 and 1900 kg of permanent magnets.

- In the case of Saturated Variable Reluctance Machines (SVRMs), the Shear Stress is in a similar range as that for PMSMs. Although the magnetic field can be higher for SVRMs (up to 1.6 T), the electric load is usually smaller ($<30 \text{ kA/m}$). Nevertheless, a great advantage of the SVRMs is its more efficient cooling and cheaper cost since their windings are concentrated.
- Another big difference is that SVRMs needs no permanent magnets that are expensive and delicate components for marine applications since they are prone to corrosion. Additionally, permanent magnets could be de-magnetised leading to a fatal breakdown because they will need to be magnetised again externally.
- The economic arguments are other point to consider. In a simple way, a conventional linear machine will be the sum, in different proportions, of three raw materials: Iron, copper and rare earth magnets. These elements need to be manipulated and transformed to its final state (cut, assembly, wound, protected, mounted, etc.). The approximate final prices for these components are in the following range [52]: Iron 3 €/kg, Copper 10 €/kg and Rare Earth Magnets 50 €/kg. Therefore, reducing the requirements of permanent magnets may also have a positive influence in the price of the machine.

Finally, these techno-economic considerations derive a conclusion: SRM can be considered a good compromised solution for a linear generator based PTO since it is simpler, more robust, more cost effective and can achieve the same controllability as any alternative machine with adequate power converters. Moreover, the linear SRM allows modular configurations. This means that once a polar structure is defined for both stator and translator, this structure can be repeated to achieve the required force and for any stroke by only modifying the length of the translator.

17.3.3.2 Introduction—Alternatives of Structure Configuration and Design of Linear Electric Machine Geometries

After the previous considerations on operation principle of the electric generator, two approaches arise to address the problem of increasing the force density, making more compact machines by means of structure configuration design:

- Increasing the airgap surface with limited impact on the machine volume
- Increasing the Shear Stress (σ).

The use of cylindrical designs is one of the possible options to increase the air gap surface in a Short-Stator configuration (CONF 6, see Fig. 17.4). Two examples of cylindrical designs are Oprea et al. [53] and Mendes et al. [54], based on PMSM and a Short-Stator SRM based on a cylindrical geometry, respectively. This structure configuration has two advantages, there are no coil ends, i.e. all the winding length produce force, and the lateral forces are fully compensated. Among the drawbacks

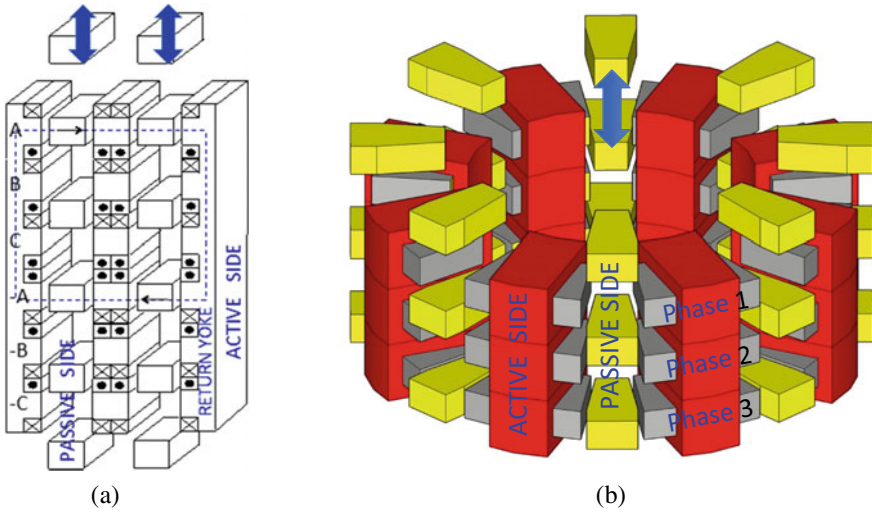


Fig. 17.11 **a** Multi-translator SRM [56]; **b** Azimuthal Multi-translator SRM [57]

can be highlighted the difficulty for placing the stator laminations in the required direction for minimising iron eddy currents, the additional iron in the axial direction of the stator to close the flux lines axially and the guidance of the cylindrical translator. Other way to increase the force density is using a multi-translator configuration (see Fig. 17.11a). This structure configuration increases by 30% the force density respect to a double-sided conventional one. It could be applied to SRM, Vernier or TFM. Finally, a new approach based on the existing multi-translator concept is shown in Fig. 17.11b. This azimuthal multi-translator SRM solution [55] aims to increase the airgap surface with reduced impact on the volume of the full machine.

The basic idea of the Rectangular Multi-translator Switched Reluctance Machine (RMSRM) shown in Fig. 17.11a is to introduce intermediate stators and translators in a Double-Sided Linear SRM. One intermediate double stator and one additional translator have been added to a conventional Double-Sided Machine with the corresponding two End Stators. Nevertheless, the Azimuthal Multi-translator SRM (AMSRM, see Fig. 17.11b) presents modifications respect to the RMSRM following the same operating principle but eliminating the return yoke and becoming all stators intermediate, without end stators. As explained before, the idea is to arrange the stator coils (active side) and the translator poles (passive side) circumferentially in a kind of toroidal geometry.

Table 17.5 shows a comparative study, which summarizes the Stator Force Density for the mentioned topologies respect to the coil depth. The benchmark case is set as the Double-Sided SRM. The results for the Single-side LSRM shows a smaller overall force density when the translator is included. Moreover, the results for the RMSRM are obtained for one intermediate stator. If this number is increased, the force density will be augmented.

Table 17.5 Relative stator force density for different LSRMs referred to the double-sided solution

	Single-sided LSRM	Double-sided LSRM	RMSRM	AMSRM
Relative stator force density	1.00	1.00	1.33	2.00

Table 17.6 Comparison of the RMSRM solution versus the AMSRM configuration

Parameter	RMSRM	AMSRM
Electric Load (A/m)	26,000	30,000
Magnetic load (T)	1.5	1.5
Shear Stress (σ) (kN/m²)	19	27
Air gap surface (m ⁻²)	8.8	37.5

Finally, the Azimuthal Multi-translator Switched Reluctance Machine has several advantages over the rest of SRM topologies:

- There are no lateral stators, and the required amount of iron is minimum, increasing the force density. This idea is to create an azimuthal flux path, closing the flux through identical Intermediate Stators, eliminating the end stators.
- The leakage flux is smaller than in the RMSRM configuration, so more force per ampere-turn can be achieved than in the equivalent RMSRM.
- Its circular arrangement is more suitable for fitting in the typical configuration of HPA, since the PTO is usually hosted in a cylindrical vessel. The azimuthal geometry has higher filling factor than the rectangular one.
- The benefits of an azimuthal configuration are increased with the square of the external diameter since air gap surface is proportional to this geometrical value.

These advantages conclude that the AMSRM configuration increases the Shear Stress (σ), which comes from a higher current density and a better magnetic circuit design. In addition, the AMSRM configuration increases the air gap surface, which is a direct consequence of the configuration of the new machine and the adaptation to the PTO shape. Table 17.6 presents a comparison between a RMSRM and an AMSRM pre-designed for a wave energy application.² These parameters summarize the improvement in the overall force and force density. Both machines have equal overall stator length, pole pitch (λ) and magnetic load. The comparison extracts that the AMSRM topology requires smaller pole depth as RMSRM, showing also better thermal performance. Therefore, its better cooling allows increasing the current density from 3.5 A/m² of the RMSRM to 4.5 A/m² in the AMSRM topology.

² The results are based on a preliminary electromagnetic design applying the methodology carried out in H2020 project SEATITAN (ID: 764014).

17.3.3.3 AMSRM Working Principle

Once AMSRM has been selected as a promising linear generator candidate, this section describes in detail its operating principle. As described before, the SRM operating principle is based on a stepper motor, where the stator phases are energising sequentially to obtain energy in generator mode or to produce energy when motoring. When the energized stator poles and the corresponding translator poles try to align, producing a net force which can act in the same direction of motion (motor operation) or opposite to it (generation). This sequential process is shown in Fig. 17.12. For a linear SRM.

Figure 17.12a describes the motor mode, in which the green phase is activated in the fully misaligned position. In this case, the pole (P) tries to align the green phase in order to minimize the reluctance of the circuit. This process generates an electromagnetic force in the same direction of the translator movement. When the pole achieves the fully alignment position, the phase is switched off and the next one is activated, in this case the yellow one. The generator mode is analogous; the phase is activated when the pole (P) is in the fully alignment position. The translator is moving towards the fully misaligned position due to an external force that pulls the translator. In this movement, an electromagnetic force due to the phase activation acts in the opposite direction of the velocity trying to brake the motion. When misalignment is achieved, the phase is switched off and the next one is switched on, in this case the yellow one.

The energisation of a SRM phase is related to the inductance evolution for each phase. The inductance changes as the translator is moving, being maximum at the fully alignment position and minimum at the fully misalignment situation. The evolution of the inductance respect to the SRM translator pole position, is shown in Fig. 17.13a. Based on this curve, two working zones are deduced related to the two operating modes. The motor mode is applied in the zone with positive slope ($dL/dx > 0$) of the energised phase, accelerating the translator since the force is positive, as Fig. 17.13b shows. However, in the generator mode, the objective is to brake the translator transforming mechanical energy into electrical one. Therefore, the phase which has a translator pole near fully alignment position and moving to a fully misalignment one is energised, corresponding to the zone with $dL/dx < 0$.

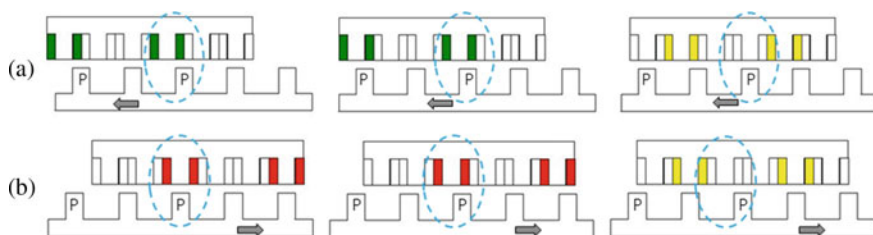


Fig. 17.12 Working principle of the LSRM: **a** Motor mode **b** Generator mode

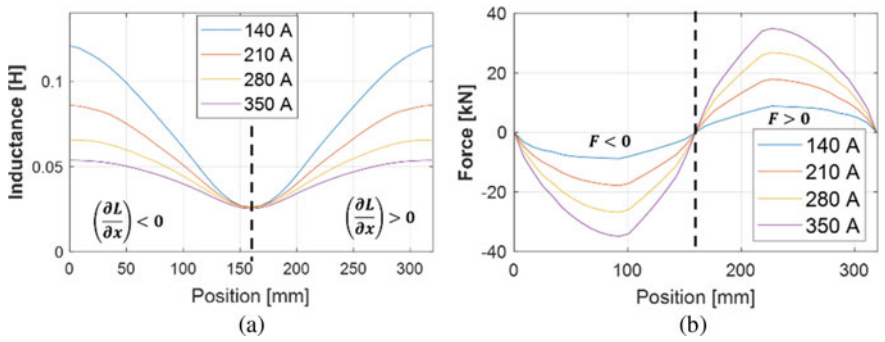


Fig. 17.13 Example of LSRM characteristics as a function of the position: **a** Inductance and **b** Force

The legend of the images shown in Fig. 17.13, shows the variations of the force and inductance as a function of the current supplied on the phases.

According to that two zones, the phase activation sequence of the SRM is shown in Fig. 17.14. In motor operation mode, phases are activated with positive slope of the inductance as a function of the position. However, the phases are switched on with negative slope when the machine works in a generator mode. Figure 17.14 represents an ideal situation since the current waveform shown is rectangular, settling and cancelling instantaneously. In a real case, the current cannot be established

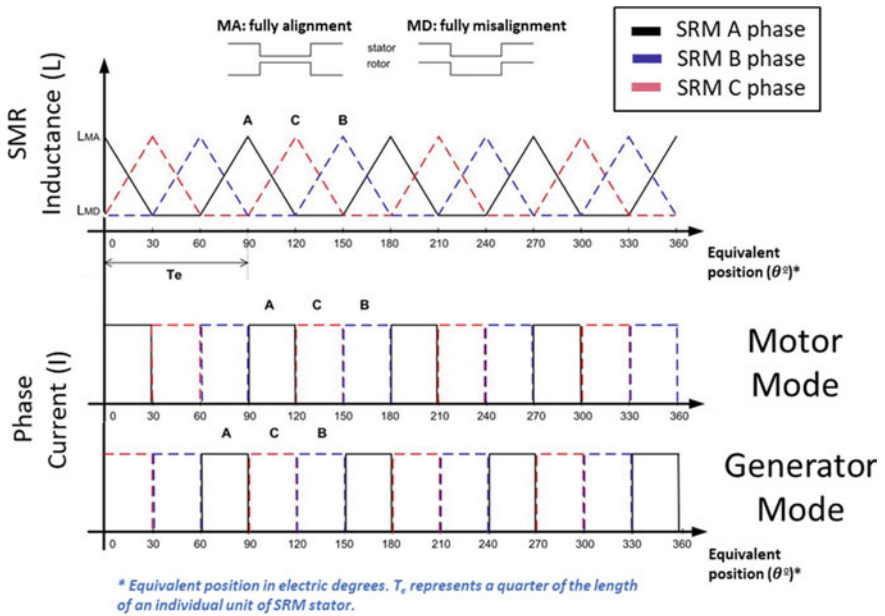


Fig. 17.14 SRM phase activation sequence

instantaneously, and therefore, currents of phases will overlap, being necessary to carry out a forward and delay to the activation positions of the phases respectively. A constant force is achieved in permanent regime thanks to the overlapping and current control.

A SRM electromagnetic model can be set out based on the next assumptions:

- Mutual magnetic coupling between phases is negligible.
- Losses by hysteresis and parasitic currents in magnetic circuit are negligible.
- Resistance of each phase is constant and independent of current frequency.
- Translator moves with negligible viscous friction coefficient.

Under these assumptions, the operation of the SRM can be described by a set of equations, one for each SRM phase. The instantaneous voltage in the phase terminals can be obtained from Faraday's law like it is shown in (1).

$$u = R \cdot i + \frac{d\phi(x, i)}{dt} = R \cdot i + \frac{\partial\phi(x, i)}{\partial i} \cdot \frac{\partial i}{\partial t} + \frac{\partial\phi(x, i)}{\partial x} \cdot \frac{\partial x}{\partial t}; \left(v = \frac{\partial x}{\partial t} \right) \quad (17.1)$$

$$\frac{di}{dt} = \frac{u - R \cdot i - \frac{\partial\phi(x, i)}{\partial x} \cdot v}{\frac{\partial\phi(x, i)}{\partial i}}; \quad (17.2)$$

where, $R[\Omega]$: electric resistance of the coils of one phase; $t[s]$: time; $i[A]$: electric current flowing in a SRM phase; $x[m]$: relative position between the active and passive parts of the SRM; $\phi(x, i)[Wb]$: Magnetic flux through the coils.

From (17.1), the evolution of the current on a phase of a SRM can be derived. Integrating (17.2), the current as a function of the time can be obtained. Finally, the electromagnetic parameters of the SRM—force and magnetic flux—are obtained by means of a finite element tool. Figure 17.15 shows an example for a SRM, presenting force, magnetic flux and the derivative terms of magnetic flux as function of current and translator position. Those data maps are tabulated and used in the mathematical model together with (17.2) to calculate the evolution of the current on each phase.

17.3.4 SRM Power Electronics and Control

17.3.4.1 Introduction

A complete DDPTO encompasses the linear electric machine, the power electronics (PE, which interconnect the electric grid with the electric machine), and the associated control [24]. In addition, it is worth mentioning that the SRM only works driven by a PE converter in order to activate/deactivate its concentrated coils in the proper sequence [58]. The PE and the control of a LSRM is described in this section.

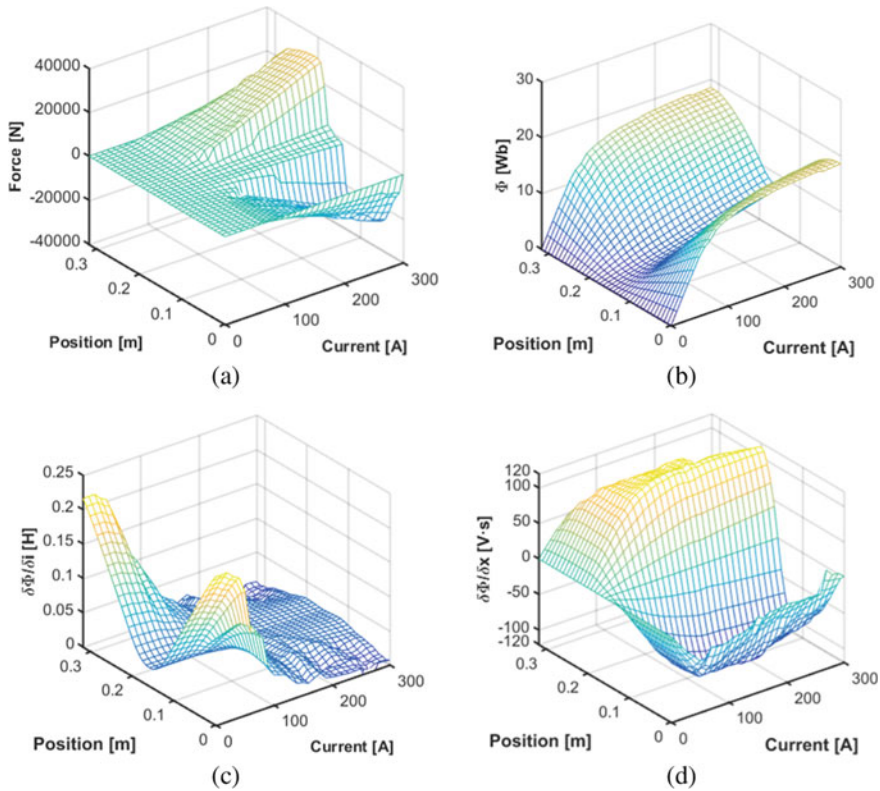


Fig. 17.15 Electromagnetic parameters of a SRM as a function of the position and current: **a** Force; **b** Magnetic flux; **c** and **d** derivative terms of the magnetic flux

One of the priority topics highlighted in the Strategic Research and Innovation Agenda for Ocean Energy [7] is the “*Improvement and demonstration of PTO and control systems*”, and one of the remarked actions is “*Optimisation and simplification through standardisation, modularity and scalability of key PTO components*”. The proposed LMSR, PE and control match this requirement.

The PE can be differentiated in two types of converters: the Linear Generator Side Converter (LGSC), which controls the energy extracted from the waves by means of the control over the linear generator; and the Electric Grid-Tie Converter (EGTC), which injects the generated electric energy in the electric grid. Nowadays, EGTC can be equipped with advanced grid functionalities such as synthetic inertia or frequency fast response, being called grid-forming converters [59].

In terms of PTO modularity (see Fig. 17.16), one LGSC module can drive serial associations of several LSRM modules. The rated current of the LGSC module is the rated current of the LSRM module, and the rated voltage is the multiplication of the LSRM module rated voltage by the number of modules in the LSRM association. In turn, one EGTC can manage parallel associations of LGSC modules. Therefore, the

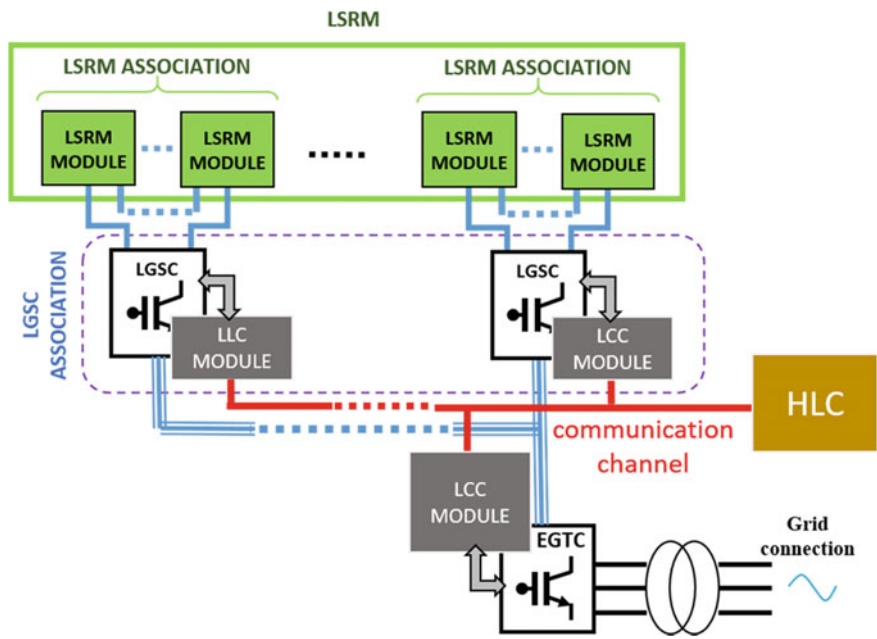


Fig. 17.16 Example of modular PTO scheme (one LGSC association/one EGTC)

rated voltage of the EGTC module is the rated voltage of one LGSC module, and the rated current of the EGTC equals the rated current of one LCSG module multiplied by the number of modules in the LGSC association. The way to associate the LSRM modules and the LGSC modules is a compromise solution between the voltage and current to be managed by the PE converters.

- Two types of control can be identified in the control loop (see Fig. 17.17):
- High Level Control (HLC), which controls the mechanic variables of the WEC, defining a force command. The aim of this control loop is to maximise the energy extracted from the waves.

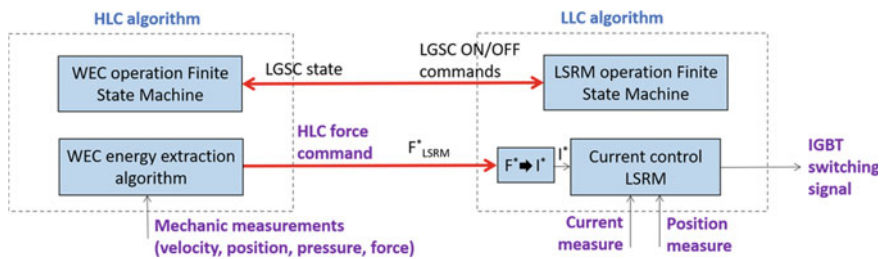


Fig. 17.17 Example of LLC/HLC scheme for the PTO

- Low Level Control (LLC), which drives the LSRM by controlling its electric variables by means of the state of semiconductors. The objective of this control loop is to impose the command force defined by the HLC.

The proposed LLC is modular, one for each PE converter module since the LLC drives the PE. The proposed HLC is unique, driving the global mechanic variables of the WEC. The modular distributed control would be interconnected by a common communication channel with an industrial field bus such as CAN or MODBUS.

The EGTC would be a common three-phase voltage source inverter [60]. The LGSC is specific, in terms of power electronic converter topology and LLC, for a LSRM. The complete electric drive, encompassing the LSRM, the power electronics and the LLC is described in Sect. 17.3.4.2.

17.3.4.2 SRM Electrical Drive: Power Electronics Topology, Control Algorithms and Operation

The LGSC must achieve a series of requirements to operate the LSRM, namely:

- Each phase of the LSRM must be independently controllable.
- The LGSC must be able to limit the current at low velocities by switching the voltage applied to the phases (i.e. hysteresis band control).
- The LGSC must be equally capable of energising the LSRM phases at rated current before entering its region of motor force.
- In the same way, the LGSC must be able to energize the next phase before the phase that has just been deactivated is completely de-energised, so that power can be extracted from several phases at the same time, reducing the force ripple.
- For the switching periods to be small, the converter must be able to energize and de-energize each phase in a very short time. This requires sufficiently high phase activation and de-activation voltages. However, the phase activation frequency in the wave energy case is not as high as in high-velocity applications [61].
- The converter must allow the free flow (freewheeling) of the current in order to reduce the switching frequency. A path of free circulating current is a so-called “zero voltage” current loop, which does not include the DC bus and applies a zero to the generator phase to rise its current with a smaller time derivative (di/dt).

To extract the energy from waves it is necessary to regulate the current at each one of the generator phases. In this case, the current through the phases of the electrical machine is unidirectional, so, by applying different voltages in the phases, it is possible to regulate this current value [58]. There are different strategies to control the current through the phases of a LSRM: hysteresis band strategy, closed-loop pulse width modulation (PWM) and direct torque control [62]. In this case, a hysteresis band strategy is proposed, which will be described in detail in Sect. ‘[Switching Strategy for Current Regulation](#)’.

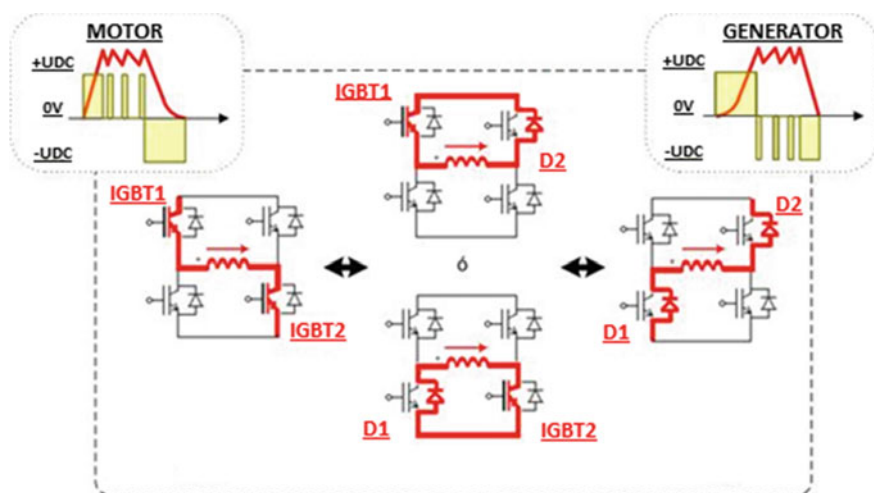


Fig. 17.18 State of the semiconductors and current flow through them in motor and generator mode for a phase of a switched reluctance machine

Switching Strategy for Current Regulation

The LGSC, which connects a DC link (U_{DC}) with an electrical machine, must be able to regulate the current through the phases of the machine. Figure 17.18 shows the status of the switches for the different voltages applied in the case of selecting an asymmetric half-bridge converter (see Sect. [Topologies for the Linear Generator Side Converter \(LGSC\)](#)).

At the beginning of the activation period of one phase $+U_{DC}$ is applied to rapidly increase the current from zero to the reference value and 0 V and $-U_{DC}$ is used alternately to keep the current within the reference band. Finally, $-U_{DC}$ is applied to extinguish the current at the end of the activation period of each phase. At low and medium velocities, when the counter-electromotive force (EMF) is not very high, current regulation is achieved by soft switching applying 0 V to increase the current within the band. This switching mode is known as ‘soft switching’ since, when the current is within the limits of the band, 0 V is applied to raise the current.

An alternative to increase the current in this situation is to apply $+U_{DC}$ instead of 0 V . This switching mode is known as ‘hard switching’. By applying $+U_{DC}$, the current increases faster than with 0 V . From the point of view of the converter losses, this mode is worse than soft switching because the switching frequency of the power converter increases. In general, hard switching is only suitable when a small hysteresis band width is required to minimize the current ripple and, therefore, when it is necessary to make the current evolve very fast.

From the point of view of the state of the switches, there are two possible combinations to apply 0 V . The two possibilities are closing either IGBT1 or IGBT2. In case of closing IGBT1, the current will circulate through IGBT1 and D1, and if

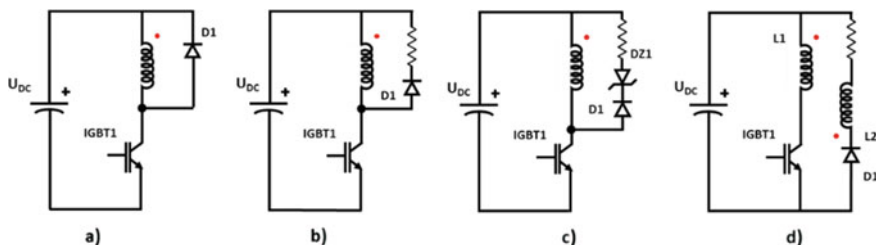


Fig. 17.19 Different topologies of LGSC converters with one switch per phase

IGBT2 is closed, the current will circulate through IGBT2 and D2 (see Fig. 17.18). A possible switching strategy consists of toggling IGBT1 and IGBT2 in each activation period to apply 0 V, so that one cycle closes IGBT1 and IGBT2 is used in the next period (cyclic soft switching). An alternative is to change IGBT1 and IGBT2 in each switching event within an activation period (alternating soft-switching).

Topologies for the Linear Generator Side Converter (LGSC)

Three main topologies of converters can be identified to drive an SRM:

(a) Power converters with one switch per phase

One switch per generator phase is enough to provide unidirectional current to the phases of the generator. Four different configurations are shown in Fig. 17.19. In the case of the topologies in Figs. 17.19a–c, the energy supplied to the magnetic field during phase activation is not returned to the source (DC link), but rather dissipated in the elements of the free circulation circuit, resulting in an inefficient option. This does not occur for the topology in Fig. 17.19d, where each phase of the machine is formed by a double winding (two windings per phase, L1 and L2), so, when the switch is open, the current through the primary winding is transferred to the secondary winding and flows through the diode. However, the drawbacks of this topology are the losses in copper associated to the auxiliary winding, and also the blocking of $2 \cdot U_{DC}$ voltage by the phase switch during the off state (double value than in the previous cases).

An extended family of power converters with a single switch per phase is represented by the “C-dump” converter shown in Fig. 17.20 [63]. The main idea of this family is to create a second voltage bus (capacitor C in Fig. 17.20) to reverse bias the phases during de-energisation after de-activation. The voltage level in this second bus is regulated on $2 \cdot U_{DC}$ by means of a DC/DC converter implemented through the switch IGBT4 and the inductance L4. This value is chosen to be able to apply a voltage of $-U_{DC}$ to the de-activated phase for rapid demagnetisation. In this sense, the main switches must be sized for $2 \cdot U_{DC}$ since it is the voltage to be blocked. In this case, the energy supplied to the magnetic field is returned to the source. The great disadvantage of this type of converters lies in the need for an additional power converter, which increases the difficulty of the PE control.

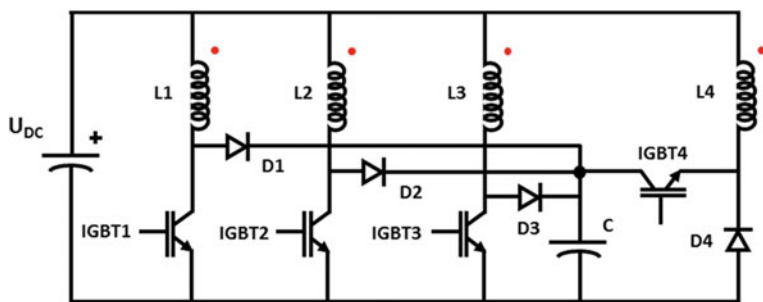


Fig. 17.20 C-dump power converter for three phases LSRM

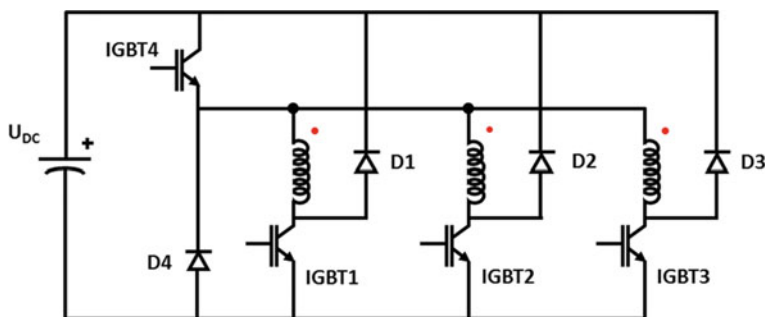


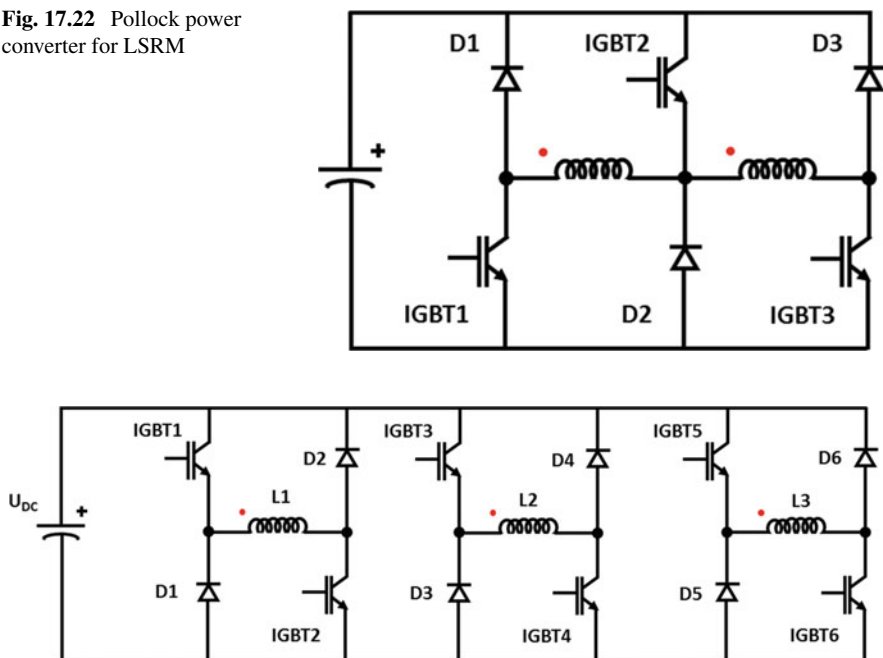
Fig. 17.21 Miller power converter for 3 phases LSRM

(b) Power converters with shared switches

There are other topologies which share switches between one or more phases, thus reducing the number of components and thus the cost of the converter. This is the reason why converters such as the one in Fig. 17.21, called “Miller” converter or “ $n + 1$ ” switch converter, have emerged [64].

In this circuit, the number of switches is one more than the number of phases of the machine. One of the switches, the upper IGBT4, is shared between all phases. To activate one of the phases, this upper switch and the lower switch are closed in series with the corresponding phase. The regulation of its current can be done either by hard-switching using both switches, or by soft-switching since various possibilities of free flow of current are offered. To de-energize the phase after de-activation, both switches are opened applying $-U_{DC}$ to the phase, thus returning the magnetic energy to the source. The limitation of this PE absence of independency in the control of the different LSRM phases, since the next phase to be activated cannot be energised until the phase that has just been de-activated is completely de-energised (since the common switch is being used to apply reverse voltage to the off phase).

There are variations of this converter, such as the Pollock converter [63], whose topology is based on the block in Fig. 17.22. As extracted from Fig. 17.22, adjacent phases of the converter share one of the switches; this considerably reduces the

Fig. 17.22 Pollock power converter for LSRM**Fig. 17.23** Power converter topology for three phases switched reluctance machine

number of semiconductors, however limits the independent control of the phases. If the two SRM phases that share a switch are activated consecutively, the next phase cannot be energised until the current in the previous phase is extinguished (since the shared switch is open to de-energize). Therefore, this topology is more convenient for SRM with a high number of phases, where the distribution of the windings in the converter can be established so that consecutive phases do not share elements. It should also be mentioned that shared switches have a higher average switching frequency and therefore will present higher losses than in other topologies.

(c) Asymmetric half bridge power converter

In this type of PE converter, each LSRM phase is in series with the switches [60]. To increase reliability and apply optimised strategies, more than one switch per phase is used. In this way, there is a full bridge converter for each LSRM phase (composed of two switches and two free-wheeling diodes), as shown in Fig. 17.23.

The upper and lower switch of each phase can be controlled independently to give rise to different switching schemes. To apply $+U_{DC}$ to each phase, IGBT1 and IGBT2 switches are closed; to apply 0 V, either IGBT1 or IGBT2 are closed; and for $-U_{DC}$, no switch is closed. This converter offers great control flexibility since the current can be treated completely independently in each phase. It also provides extra reliability to the LSRM PTO, since it avoids a short circuit of the DC bus through the main switches, as the phase winding is connected in series between both semiconductors.

Table 17.7 Comparison of the power converter topologies for LGSC

Topology	Power converter configurations	Advantages and drawbacks
One switch per phase	1: One switch per phase (Fig. 17.19a–c)	<u>Cons.</u> : It is not possible to recover the energy supplied during the activation of the phase, low efficiency, and low versatility <u>Adv.</u> : Reduced number of components and low cost
	2: One switch per phase (Fig. 17.19d)	<u>Cons.</u> : Low efficiency due to power losses in the secondary winding, the blocking of 2-UDC voltage by the phase switch and higher complexity <u>Adv.</u> : Low cost
	3: C-dump power converter	<u>Cons.</u> : Complexity in control, an additional power converter and high cost <u>Adv.</u> : Recovery of the energy supplied during the activation of the phase
Shared switches	4: Miller power converter	<u>Cons.</u> : No independence in the control of each phase and high current ripple <u>Adv.</u> : Reduced number of elements and low cost
	5: Pollock power converter	<u>Cons.</u> : Higher average switching frequency and no independence in the control of each phase in machines with low number of phases <u>Adv.</u> : Reduced number of components and low cost
Half bridge	6: Asymmetric half bridge power converter	<u>Cons.</u> : High number of elements and higher cost. <u>Adv.</u> : Independence in the control of each phase, higher control flexibility and lower current ripple

Furthermore, all switches and diodes must be sized for the same U_{DC} voltage. The main drawback of this topology is the greater number of switches required. Also, for low voltage applications, the voltage drop across the two semiconductors can be significant relative to the DC bus voltage. However, this converter is optimal for medium/high voltage applications where performance is critical and, for all its advantages, it is widely used for LSRM applications.

(d) Summary

As a summary, the following comparative table is proposed (Table 17.7). From the topologies presented in the table, a particularly suitable topology is PCT 5 because,

despite the greater number of semiconductors, it allows independent control of the current of each phase.

Usually, the linear electric machines are designed with wider airgaps that conventional rotary machines due to the long displacement strokes, and this issue leads to a limitation in the maximum slope of the current evolutions. In order to a proper control of the phase currents, it is necessary overlap the activations of the phases, and hence, a power electronic converter capable to control independently the current in each phase.

Control Techniques to Reduce the Torque Ripple in LSRM

As mentioned in Sect. 0, the SRM has a high ripple in force when compared to other types of electrical machines. There are two types of techniques to minimise the force ripple, related either to modifications in the machine topology or to the power converter control strategy. This section describes different existing techniques based on control strategies. The main existing techniques are listed below:

(a) Current and angle modulations

Traditionally, there have been two different ways of reducing torque in switched reluctance machines from a control point of view: the on-off angle optimisation method and the method for following a certain current profile. The first one consists in optimising the angles to achieve a certain torque. However, this method fails to accurately master the behaviour of the torque. The second of the methods consists of following a certain current reference that achieves a certain torque reduction. The drawback of this method is that it is necessary to store a large amount of data to know the exact current value in each situation to give a certain torque value. This method is proposed in [65]. Another additional method derived from the previous one consists of the independent control of the current in each of the poles [66].

(b) Average torque control and Direct torque control

A new scheme for the control of the mean torque in reluctance machines is proposed in [67]. The average torque control (ATC) technique can be implemented using the online average torque and energy ratio estimation method for closed loop control. The torque reference varies constantly as a function of the commutation angles and the reference current to achieve a constant average torque given as the reference value. Due to the adaptive adjustment of the system parameters, precise torque control and acceptable reduction in torque ripple are obtained.

The technique known as direct torque control (DTC) has been employed to minimize torque ripple in SRM [68]. The value of the reference current is obtained from a look-up table in which the position of the moving part of the machine, the torque and the current are related. Semiconductor trigger signals are obtained by comparing the current reference value and the measured value. There is another control technique derived from the previous one called instantaneous torque control (DITC) that achieves a faster response in reducing the torque error [69]. The torque

measured is estimated online and the semiconductor trigger signals are the result of a hysteresis band control of the torque. Another technique of instantaneous torque control regulating the reluctance co-energy of the machine is proposed in [70].

(c) Torque sharing function

Another control technique to reduce the torque ripple is the torque sharing function (TSF) with the hysteresis band current control. The reference torque can be defined by a TSF, where the sum of the torque references of each of the phases is equal to the reference of the output torque. The torque of each phase is obtained from the predefined torque profile in a look-up table that relates current, position of the moving part of the machine and torque. The total reference torque of the machine is divided by the number of phases of the machine depending on the position of the machine and as many torque references as phases of the machine are generated. Once the position of the machine and the torque reference are known, the reference currents through the phases of the machine are generated. The reference currents are compared to the measured currents and the switching signals are generated by a hysteresis band control. This method allows to smooth the torque shape, avoiding torque peaks that cause a high ripple. Torque peaks occur during the activation switching of each phase, so there are advanced TSF techniques to minimize torque ripple in these transitions and obtain a better response [71].

(d) Feedback linearisation control, Iterative learning control and Intelligent control

Other techniques used to reduce torque ripple are: feedback linearisation control (FBL), iterative learning control (ILC) and intelligent control (IC). FBL uses a feedback linearisation controller to achieve a closed-loop linearised system. This loop makes it possible to compensate for the non-linear behaviour of the reluctance machine [72]. ILC is an appropriate control technique for non-linear systems with many coupled variables and in which a very precise analysis of the model is required without the need to identify the machine parameters. This method consists of an iterative process in which the necessary waveform to give a certain torque and the voltage that must be applied to the machine phase to achieve that waveform are determined [73]. Finally, IC is based on the use of techniques such as neural networks, or fuzzy logic. This method has a great adaptive capacity and robust self-learning. It is based on the use of a precise estimation of the torque from the voltages and currents measured in the phases of the machine. The estimated torque is compared with the reference torque and the controller based on one of the optimisation techniques discussed generates the reference currents in the machine phases [74].

Multimode Hysteresis Band for LSRM Current Control

As explained in the previous Sect. ‘[Switching Strategy for Current Regulation](#)’, the proposed current control for the LSRM consist in a hysteresis-band soft-switching strategy. However, at low velocities, the low values of EMF (electromotive force) cannot drive the LSRM current. In particular, according to the SRM phase Eq. (17.2),

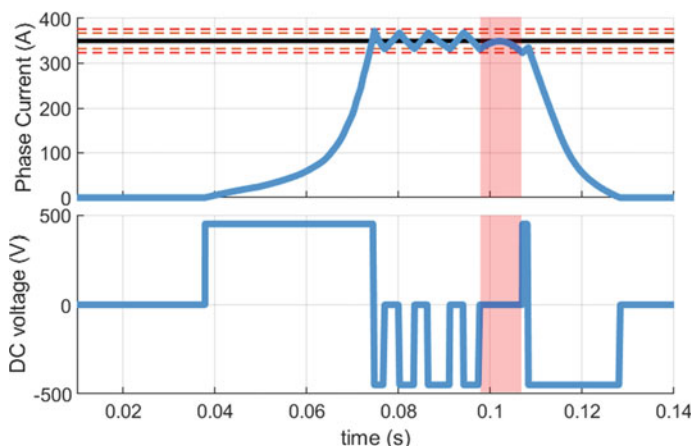


Fig. 17.24 Example of LSRM current with a bad estimation of the velocity limit

If 0 V is imposed when the LSRM is working as a generator, the current evolution depends on the value of the velocity. The current slope is positive at high velocities, as expected in a generator mode. The current slope is negative at low velocities, as it occurs in motor mode due to the LSRM is operating in a non-regenerative generator working point.

A velocity value delimits each LSRM current behaviour, and this limit value depends on the current. In the case of wave energy extraction, the velocity of the electric drive changes of sign in every wave cycle and, hence, the two LRMS current behaviours occur and they must be taken into account. One solution is the use of a ‘multimode soft-switching hysteresis band’ [75]. This hysteresis-band soft-switching strategy drives the current by applying:

- A generator mode commutation when the velocity is upper than the velocity limit: $[0 \text{ V}/-U_{DC}]$ pair to increase/decrease the current respectively.
- A motor commutation mode when the velocity is lower than the velocity limit: $[+U_{DC}/0 \text{ V}]$ to increase/decrease the current respectively.

An accurate calculation of the velocity limit value for each current would be required for the multimode operation. For this reason, an external hard-switching hysteresis band is establishing in order to manage incorrect estimations of the velocity limit values at each current. Figure 17.24 shows an example of the LSRM current behaviour with a bad estimation of the velocity limit. In the last part of the phase current evolution, the slope of the current changes sign without a change in the switching state. Figure 17.25 shows a scheme of the current behaviour when a multimode soft-switching band is applied, including the hard-switching external band.

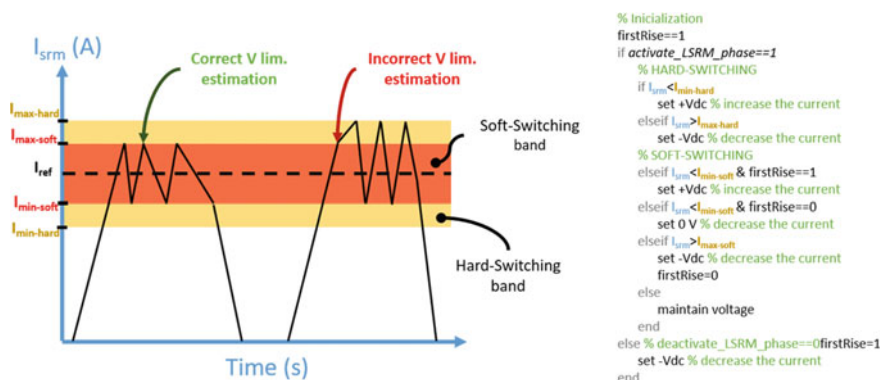


Fig. 17.25 Scheme of the multimode soft-switching hysteresis band (left). Pseudocode of multimode soft-switching hysteresis band (right)

17.4 Superconducting Linear Switched Reluctance Machine (LSRM)

17.4.1 Introduction

As explained in previous sections, there are a number of different approaches to harvest energy from the ocean waves. As shown in Sect. 17.2.2 the approach can be summarised on 10 types of different technologies, with the Point Absorber as the most common one, being present in 33% of those devices. The Oscillating Water Column and the Oscillating Wave Surge Converter Pressure Differential were selected in the 6% and 3% of the devices, respectively. One of the characteristics that these three technologies have in common (since they are based on a linear displacement between two bodies) is that they are very suitable for using DDPTOs to perform the energy conversion process as they are linear displacement devices with a single conversion stage of energy, which makes them very efficient.

At the same time, it is quite intuitive that the forces required in this conversion process are very high. For instance, for a 10 s period wave of 2 m in amplitude the peak vertical velocity would be 0.4 m/s. If a peak power of 1 MW is required, a peak force of 2.5 MN would be needed (only considering the active force component, although in some devices an additional reactive force is required). When talking about such big forces for an electrical machine, superconductivity becomes an interesting option to be considered. Ultimately, a high force machine means a high current machine for what a superconducting option can be almost indispensable. Besides, there is an additional consideration in favour of a superconducting version which is the higher efficiency, something which is also indispensable to harvest energy when high reactive forces are involved.

17.4.2 *The Importance of High Force/High Efficiency PTOs*

To analyse the convenience of a superconducting PTO let us consider the case of the Heaving Point Absorber (HPA), which, as it has been already explained, is based on the relative movement of two bodies: One is stationary or pseudo-stationary and it is called the Spar, while the other is moving and it is called the Float. To analyse the impact on the requirements of the PTO force and efficiency, we will consider the real WEC example already presented in Sect. 17.3.2 (UNDIGEN W1 prototype [36]). The results were presented in Fig. 17.8a (100% of efficiency, 1 MN PTO) and Fig. 17.8b (75% of efficiency, 1 MN PTO). There are two main conclusions that can be extracted from Fig. 17.8b (75% of efficiency PTO):

- Only for a very narrow window of wave periods, the maximum available power (red curve) can be extracted. For the rest of periods, the power that can be harvested (yellow curve) is very small.
- The force that the PTO uses to produce power (green curve) is below the maximum available force to avoid increasing the losses above the extracted power and, in any case, it is much below the required force to extract the maximum power (blue curve).

If we now use an ideal superconducting PTO with the same force (1 MN) but an efficiency of 100%, alternative results are obtained (see Fig. 17.8a) and another two important conclusions can be extracted:

- The window for which the maximum theoretical limit can be extracted becomes much broader.
- All the available force is used until the required force is bigger than what the PTO can provide, and the extracted power is unable to follow the maximum power path. If we make a more powerful PTO, we should be able to follow the maximum power curve up to the required wave period.

Superconducting PTOs become then a very convenient alternative to increase the area of the Power versus Wave Period curve, making it closer to the maximum magnitude that can be theoretically achieved. Both, the increasing of force capability and the improvement of the efficiency contribute to this increment.

17.4.3 *Some Simple Concepts on Superconductivity and Cryogenics*

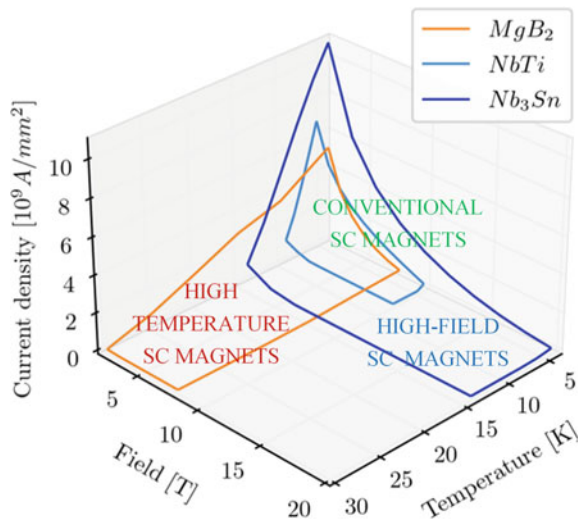
Superconductivity is the property that some materials present under certain conditions to transport electrical current without losses. In other words, the absence of electrical resistance. Besides this fact, two other phenomena characterize the superconducting state: Diamagnetism (*Meissner Effect*) and a finite leap in the specific heat curve. The explanation of superconductivity as well as its physical details are far away

from the scope of this introduction, but some useful concepts should be mentioned here. As previously said, the superconducting state only occurs under certain conditions which can be expressed in a simple manner [76]: The point defined by the following three coordinates: the current density flowing through the superconductor (J), the magnetic flux density (B) in which it is immersed and the temperature (T) at which it is working, must be inside a volume which is defined by the intersection of the so-called critical surface with the coordinate planes. The intersection of the critical surface with the J , B & T axes define the critical values: Critical J (J_c), Critical B (B_c) and Critical T (T_c).

There are two big groups of superconductors attending, basically, to the value of their critical temperature. The first group constitute the Low T_c Superconductors with critical temperatures below 20 K, which are mostly intermetallic alloys and obey to the BCS theory to explain the mechanism of superconductivity. There is an exception within this group which is the MgB_2 (Magnesium Diboride) [5] with a critical temperature of 39 K, a non-metallic compound which also obeys to the BCS theory. Figure 17.26 shows the critical surfaces for the three most relevant superconductors of the previous group. The other group is called High T_c Superconductors with critical temperatures above 70 K. They are ceramic materials based on copper oxides and a rare earth element and their superconductivity is not explained by the BCS theory. Figure 17.26 also shows the area of operation for different types of superconducting magnets, including conventional ones, high field ones and those working at higher temperatures but moderated fields. For each type, a different type of superconductor becomes more suitable.

Superconducting wires are able to transport current densities which can be easily two orders of magnitude higher than those for normal conducting wires and this implies a significant reduction in the size of the devices but also in their power

Fig. 17.26 Critical surfaces for NbTi, Nb_3Sn & MgB_2



consumption. In this manner, they are especially adequate for magnet manufacturing in general and for electrical machine windings in particular, which can be considered as a special case of magnets. Nevertheless, superconductivity has two big issues to overcome:

- While the resistance is null for direct current (DC), when transporting alternate current (AC) there are losses associated to the induced electric fields in the superconductor. Besides, there are also dissipative currents induced in the metal matrix in which the SC material is allocated. The consequence is that both terms heat up the material driving it to the normal state. This fact limits the application of superconductors to DC or to low frequency ones and requires the use of special wires based on very small filaments of SC material and high electrical resistance matrices [77]
- The magnet has to operate at cryogenic temperatures (in the order of 10 K or less) and this requires a complex cryogenic facility to cool the magnet down but also to keep it cold.

Usually, cryogenic aspects of superconductivity are even more complex than the superconducting aspects themselves. To cool the magnet down there are different possibilities spanning from submerging it into a liquid coolant as helium, circulating a coolant liquid or a gas through it or extracting the heat from the magnet by conduction using a cryocooler [78]. To keep it cool, the magnet must be thermally insulated from outside, minimising the heat which is conducted and radiated. For the first case the magnet must be in a vacuum atmosphere (typically 10–6 mbar) while for the second one, the solution is to shield the magnet with a screen that reduces the radiated heat to the outer wall of the vacuum chamber. In any case, it becomes essential to reduce the losses associated to the magnet to the minimum possible value since, extracting 1 W at 4.2 K implies a real power consumption of some kW at room temperature (significantly higher than the theoretical Carnot limit). In this sense, increasing the operational temperature of the superconductor has a great impact on the overall design, either because the refrigeration power is reduced or because the requirements of thermal insulation are not so strict.

17.4.4 Options for Superconducting Machines: A Superconducting PTO

Theoretically, every conventional machine has its corresponding superconducting version, nevertheless, the limitations associated to superconductivity, restricts the real number of types of superconducting (SC) machines that can be performed. Particularly, there are two severe restrictions to consider: (1) AC losses must be reduced below admissible values below the refrigeration system capabilities. For this reason, historically, superconducting machines only introduce SC windings associated to the DC side (2) powering SC windings that are moving and must work at

cold is very complex and this is the reason why, normally, only stationary windings are superconducting, although there are exceptions. In other words, in most of the existing realisations concerning SC machines only the excitation DC field windings are stationary and superconducting. Alternatively, solutions for using bulk superconductors as high field permanent magnets to create the excitation field in the electrical machine have also been proposed, even in linear machines [79, 80]. There are few realisations integrating superconductivity in linear machines for PTO applications. One interesting case was the one proposed by Keysan and Mueller [81, 82] which is based on a Linear Synchronous Machine with SC excitation and normal conducting stator, to avoid AC losses. The SC excitation may have homopolar or bipolar configurations and it is based on using a superconducting coil and an iron yoke to create a dipole magnetic field which crosses the copper armature windings powered by electric current. Interaction between the magnetic field and the current, creates a net thrust (action & reaction) on each side of the machine.

Generally speaking, there are three possible configurations for a linear SC machine, regarding the operational temperature of its main components. In principle there is only one condition to fulfil: SC coils must be at cryogenic temperatures; the rest can be either at cold or warm temperatures. Figure 17.27a shows the configuration where only the coils are at cold, Fig. 17.27b the configuration where all the stator is at cold (iron & coils) while the translator is warm and Fig. 17.27c shows a configuration where all the machine is cold. The big difference between them concerns the size of the air gap.

While for the first case the airgap can be as small as in any conventional machine (say in the order of 1 mm), for the second one there is a minimum airgap given by the necessary width of the cryostat which can easily be in the order of 50 mm. Finally, the third case requires an airgap of around 3–5 mm, big enough to allocate a radiation screen but much smaller than what is needed for the previous one. Apparently, the first case should be preferable to the other two cases since the airgap is the smallest of them, but there is a big issue associated to it: since each coil requires its own cryostat,

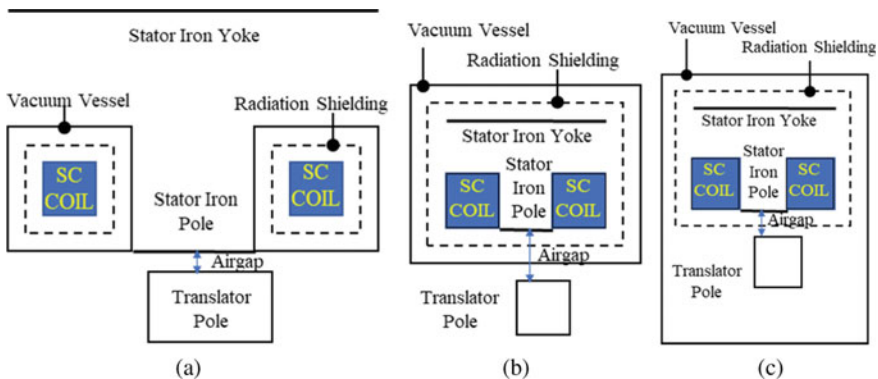


Fig. 17.27 **a** Only superconducting (SC) coils working at cold; **b** Full stator working at cold; **c** Full stator & translator working at cold

the equivalent coil size (including the coil and the cryostat) can be of the same order of magnitude as for a conventional non-SC coil. Besides this fact, the mechanical support of the coil in this solution becomes very complicated. Solution presented in Fig. 17.27b is extremely compact, and coils are directly wound around the iron making very easy their structural support; the problem now is the huge airgap which is needed and the corresponding associated stray field. Even if the ampere-turns are increased to compensate the bigger gap, the machine becomes very inefficient from a magnetic point of view. Solution depicted in Fig. 17.27c includes the advantages of the two previous ones, avoiding their drawbacks: the coil can be easily supported, retaining the big electromagnetic forces that appear, while the airgap can be small enough to guarantee an efficient magnetic design.

Figure 17.28 shows a proposal for a SC linear displacement PTO based on the third solution [83]. All the machine is allocated inside a flexible cryostat consisting of two upper and a lower bellows joined to a central stationary body where the stator is allocated and surrounded by a radiation screen. The translator is fixed to the moving parts of the cryostat but thermally insulated from them. A guiding system guarantees a rectilinear displacement. The only limitation of the third solution in general and in this proposal in particular, is the cryostat length which reduces the applications of

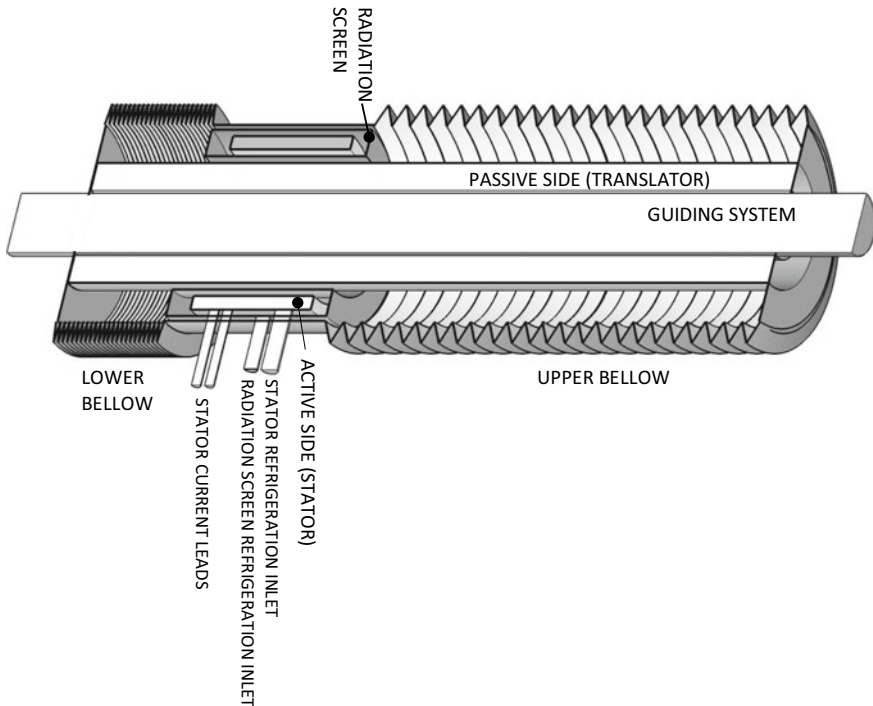


Fig. 17.28 Superconducting PTO based on a flexible cryostat

the machine to those involving a reciprocating short-medium stroke movement but not a long linear displacement.

Concerning the type of electrical machine than can be used, there are several options with the only restriction of avoiding translators with windings. Machine represented in Fig. 17.27 corresponds to a cylindrical SRM type [54] but also synchronous or permanent magnet machines can be used. In any case, the important contribution of superconductivity is the increasement of current density and, consequently, the strong growth of the ampere-turns with a similar machine size. Since, for a saturated machine, the force is approximately proportional to the ampere-turns, SC machines can easily provide forces one order of magnitude bigger than the conventional ones with similar sizes, when all the different aspect, including cryogenics, are taken into account.

17.5 Concluding Remarks

This chapter analyses the use of linear electrical switched reluctance machines (SRM) as PTO in wave energy systems. After an introduction about general concepts of wave energy conversion and a description of the direct-drive PTO concepts in Sects. 17.1 and 17.2, the chapter is focused on two main points: new electrical machine topologies; and machine developments based on superconductivity.

Respect to the first point (new machine topologies), a review of previous works related with linear electric machines in wave energy conversion are presented in Sect. 17.3 including power electronics and control issues.

In this section, a new azimuthal topology of SRM (AMSRM) is described according to Blanco Aguado et al. [57]. The azimuthal topology can be compared with a rectangular topology (MSRM), as proposed in Lucas and Pinilla [84]. The following improvements can be remarked:

- Azimuthal configuration has an advantage for a WEC PTO application, since it has a higher filling factor than the rectangular one due to the PTO is hosted in a cylindrical vessel, being much more efficient.
- AMSRM increases the Stator Force Density compared to MSRM by developing an azimuthal configuration of a Multi-translator Switched Reluctance Machine. AMSRM fully eliminates the End Stators of the MSRM topology, by creating an azimuthal flux path, closing through identical Intermediate Stators, avoiding the need of lateral iron to close the magnetic circuit.
- AMSRM reduces the machine weight since this configuration eliminates the lateral end stators, increasing the force density respect to the MSRM. Moreover, azimuthal configuration presents an airgap surface growth by a consequence of its configuration and its adaptation to the PTO shape.

The future perspectives of the AMSRMs are great since their performance increasing with their outer diameter, i.e. the force developed by the machine grows higher than the square of their surface, as shown in Table 17.8. Therefore, the higher

Table 17.8 Comparison of the force developed by three AMSRM configurations

Parameter	AMSRM Conf 1	AMSRM Conf 2	AMSRM Conf 3
No. of active sides	8	16	32
No. of passive sides	8	16	32
No. of gaps per phase	16(2mmeach)	32(2mmeach)	64(2mmeach)
Diameter (D) (mm)	1000	2000	3000
Axial length (l) (mm)	280	620	800
Height (h) (mm)	800	1056	1303
Average force @ nominal current (N)	34,293	207,424	574,529

the outer diameter, the larger the air gap surface, and with it, the force developed by the machine.

Respect to the second point (superconducting machines), it has been justified the superconductivity solution in Sect. 17.4, in addition to presenting a specific design. A Power Take-Off for wave energy extraction converters is one of the applications where superconductivity becomes more adequate in the coming years for two main reasons which are closely related: on the one hand, big forces are required to achieve significant power levels, since the moving speed is very low. Furthermore, if the PTO capability of supplying reactive force to increase the power capture ability is required, the level of needed force is even higher and superconductivity is almost indispensable if an all-electric PTO is preferred. On the other hand, big forces imply big currents which mean big losses in resistive generators that must be oversized. Besides, these losses can make the use of reactive force not efficient which, again limits extracting all the available energy for a given sea state.

In this regard superconductivity allows transporting very big current without losses which, at the end, allows increasing the operational magnetic field. Since the force is the product of the current times the magnetic field, a significant force increase can be achieved and what is even more important; a dramatic force density (force per generator unit mass) increment will happen.

A brief list and description of superconducting technologies has been presented in the chapter (Sect. 17.4) as well as the main issues that superconductivity must overcome like the A.C. losses or the cryogenic configuration to cool the magnet down to operational temperatures. It has also been shown how the way the coils are insulated in their vessels affects enormously to the magnetic efficiency and in this sense a very compact design based on cold Active and Passive Sides has been presented as an example of what could be a compact superconducting generator.

Acknowledgements This research, developed under the Project SETITAN (ID: 764014), has been supported and has received funding from European Union's Horizon 2020 research and innovation programme under H2020-EU.3.3.2.—Low-cost, low-carbon energy supply (LCE-07-2016-2017).



References

1. (2015) *International Levelised Cost of Energy (LCOE) for ocean energy technologies*.
2. Low Carbon Innovation Coordination Group. (2012). *Technology Innovation Needs Assessment (TINA), Marine Energy, Summary Report*.
3. (2013) *Ocean energy: Cost of energy and cost reduction opportunities*.
4. Iglesias, G., Astariz, S., & Vazquez, A. (2018). The economics of wave and tidal energy. In *Wave and tidal energy* (pp. 513–532). Wiley.
5. Magagna, D., Monfardini, R., & Uihlein, A. (2016). *JRC ocean energy status report 2016 edition*. Publications Office of the European Union.
6. Magagna, D., & Uihlein, A. (2015). *2014 JRC ocean energy status report*. Luxembourg: Publications Office of the European Union.
7. Villate, J. L. (2020). *Strategic research and innovation agenda for ocean energy*.
8. Magagna, D., Margheritini, L., Alessi, A., Bannon, E., Boelman, E., Bould, D., & et al. (2018). *Workshop on identification of future emerging technologies in the ocean energy sector*. European Commission JRC.
9. (2011) Accelerating marine energy: The potential for cost reduction—Insights from the carbon trust marine energy accelerator. *Technical report for carbon trust*.
10. WES|Programmes: Power Take Off. <https://www.waveenergyscotland.co.uk/programmes/details/power-take-off/>. Accessed May 27, 2020.
11. Têtu, A. (2017). *Power take-off systems for WECs* (pp. 203–220).
12. Wave devices: EMEC: European Marine Energy Centre. <http://www.emec.org.uk/marine-energy/wave-devices/>. Accessed October 12, 2015.
13. LiVecchi, A., Copping, A., Jenne, D., Gorton, A., Preus, R., Gill, G., Robichaud, R., Green, R., Geerlofs, S., Gore, S., Hume, D., McShane, W., Schmaus, C., & Spence, H. (2019). *Exploring opportunities for marine renewable energy in maritime markets*. U.S. Department of Energy (DOE).
14. Liu, Z., Zhang, R., Xiao, H., & Wang, X. (2020). Survey of the mechanisms of power take-off (PTO) devices of wave energy converters. *Acta Mechanica Sinica*, 36, 644–658. <https://doi.org/10.1007/s10409-020-00958-z>
15. (2012) *Wave dragon*. https://en.wikipedia.org/wiki/Wave_Dragon. Accessed March 11, 2021.
16. Falcão, A. F de O. (2010). Wave energy utilization: A review of the technologies. *Renewable and Sustainable Energy Reviews*, 14, 899–918. <https://doi.org/10.1016/j.rser.2009.11.003>
17. Drew, B., Plummer, A. R., & Sahinkaya, M. N. (2009). A review of wave energy converter technology. *Proceedings of the Institution of Mechanical Engineers, Part A: Journal of Power and Energy*, 223, 887–902. <https://doi.org/10.1243/09576509JPE782>
18. Moretti, G., Santos Herran, M., Forehand, D., Alves, M., Jeffrey, H., Vertechy, R., & Fontana, M. (2020). Advances in the development of dielectric elastomer generators for wave energy conversion. *Renewable and Sustainable Energy Reviews*, 117, 109430. <https://doi.org/10.1016/j.rser.2019.109430>
19. Ahamed, R., McKee, K., & Howard, I. (2020). Advancements of wave energy converters based on power take off (PTO) systems: A review. *Ocean Engineering*, 204, 107248. <https://doi.org/10.1016/J.OCEANENG.2020.107248>
20. Magagna, D. (2019). *Ocean energy technology development report*.

21. Khatri, P., & Wang, X. (2020). Comprehensive review of a linear electrical generator for ocean wave energy conversion. *IET Renewable Power Generation*, 14, 949–958.
22. Joubert, J., van Niekerk, J., Rienecke, J., & Meyer, I. (2016). *Wave energy convertors (WEC): A review of the technology and power generation*.
23. S.p.A., U. C. (2017). *ReBaS generator (Reciprocating Ball Screw Generator)—PTO Stage 2—Public Report*. UMBRA Cuscinetti S.p.A.
24. Mueller, M., & Polinder, H. (2013). *Electrical drives for direct drive renewable energy systems*. Woodhead Publishing.
25. Penalba, M., & Ringwood, J. (2016). A review of wave-to-wire models for wave energy converters. *Energies*, 9, 506. <https://doi.org/10.3390/en9070506>
26. Lin, Y., Bao, J., Liu, H., Li, W., Tu, L., & Zhang, D. (2015). Review of hydraulic transmission technologies for wave power generation. *Renewable and Sustainable Energy Reviews*, 50, 194–203. <https://doi.org/10.1016/j.rser.2015.04.141>
27. Waters, R., Stålberg, M., Danielsson, O., Svensson, O., Gustafsson, S., Strömstedt, E., Eriksson, M., Sundberg, J., & Leijon, M. (2007). Experimental results from sea trials of an offshore wave energy system. *Applied Physics Letters*, 90, 034105. <https://doi.org/10.1063/1.2432168>
28. Santos, M., Lafoz, M., Blanco, M., García-Tabarés, L., García, F., Echeandía, A., & Gavela, L. (2012). Testing of a full-scale PTO based on a switched reluctance linear generator for wave energy conversion. In *4th International Conference on Ocean Energy (ICOE2012)*.
29. Edinburgh U of C-GEN Direct Drive PTO. (2017). *PTO Stage 2—Public Report*. University of Edinburgh
30. Keller, J. (2020). *Test of a novel, commercial-scale wave energy direct-drive rotary power take-off at the NREL National Wind Technology Center: Cooperative Research and Development Final Report, CRADA Number CRD-14-571*.
31. Mueller, M. A. (2002). Electrical generators for direct drive wave energy converters. In *Proceedings of the generation, transmission and distribution* (pp 446–456). IEE.
32. Polinder, H., Mueller, M., & Scuotto, M. (2007). Linear generator systems for wave energy conversion. In *Proceedings of the 7th European wave and tidal energy conference*.
33. Elwood, D., Yim, S. C., Prudell, J., Stillinger, C., von Jouanne, A., Brekken, T., Brown, A., & Paasch, R. (2010). Design, construction, and ocean testing of a taut-moored dual-body wave energy converter with a linear generator power take-off. *Renewable Energy*, 35, 348–354. <https://doi.org/10.1016/j.renene.2009.04.028>
34. Polinder, H., Damen, M. E. C. E. C., & Gardner, F. (2004). Linear PM Generator system for wave energy conversion in the AWS. *IEEE Transactions on Energy Conversion*, 19, 583–589. <https://doi.org/10.1109/TEC.2004.827717>
35. Liu, C., Yu, H., Hu, M., Liu, Q., Zhou, S., & Huang, L. (2014). Research on a permanent magnet tubular linear generator for direct drive wave energy conversion. *IET Renewable Power Generation*, 8, 281–288. <https://doi.org/10.1049/iet-rpg.2012.0364>
36. Blanco, M., Lafoz, M., Pinilla, G., Gavela, L., García-Tabarés, L., & Echeandía, A. (2010). Electric linear generator to optimize a point absorber wave energy converter. In *3rd International conference and exhibition on Ocean Energy, ICOE 2010*.
37. Falnes, J. (2002). *Ocean waves and oscillating systems, linear interactions including wave-energy extraction*. Cambridge University Press.
38. Hai, L., Goteman, M., & Leijon, M. (2016). A methodology of modelling a wave power system via an equivalent RLC circuit. *IEEE Transaction on Sustainable Energy*, 3029, 1–1. <https://doi.org/10.1109/TSSTE.2016.2538803>
39. Falnes, J. (2007). A review of wave-energy extraction. *Marine Structures*, 20, 185–201. <https://doi.org/10.1016/j.marstruc.2007.09.001>
40. Hals, J., Falnes, J., & Moan, T. (2011). A comparison of selected strategies for adaptive control of wave energy converters. *Journal of Offshore Mechanics and Arctic Engineering*, 133, 31101. <https://doi.org/10.1115/1.4002735>
41. Joseph, D. M., & Cronje, W. A. (2007). Design and analysis of a double-sided tubular linear synchronous generator with particular application to wave-energy conversion. In *2007 IEEE power engineering society conference and exposition in Africa—PowerAfrica* (pp. 1–8).

42. Lu, Q., & Ye, Y. (2009). Design and analysis of tubular linear PM generator. *IEEE Transactions on Magnetics*, 45, 4716–4719. <https://doi.org/10.1109/TMAG.2009.2022184>
43. Nakamura, T., Nishio, H., Amemiya, N., Kajikawa, K., & Wakuda, T. (2012). Performance of induction/synchronous motor having MgB_2 cage windings for liquid hydrogen circulation pump. *IEEE Transactions on Applied Superconductivity*, 22, 5200404. <https://doi.org/10.1109/TASC.2011.2179398>
44. Ching, T. W., Chau, K. T., & Li, W. (2016). Power factor improvement of a linear vernier permanent-magnet machine using auxiliary DC field excitation. *IEEE Transactions on Magnetics*, 52, 1–4. <https://doi.org/10.1109/TMAG.2016.2524533>
45. Toba, A., & Lipo, T. A. (2000). Generic torque-maximizing design methodology of surface permanent-magnet vernier machine. *IEEE Transactions on Industry Applications*, 36, 1539–1546. <https://doi.org/10.1109/28.887204>
46. Li, J., Chau, K. T., Jiang, J. Z., Liu, C., & Li, W. (2010). A new efficient permanent-magnet vernier machine for wind power generation. *IEEE Transactions on Magnetics*, 46, 1475–1478. <https://doi.org/10.1109/TMAG.2010.2044636>
47. Lomonova, E. A., Tang, Y., Paulides, J. J. H. (2015). Hybrid-excited variable reluctance machines. In *2015 International Aegean Conference on Electrical Machines Power Electronics (ACEMP), 2015 International Conference on Optimization of Electrical Electronic Equipment (OPTIM) 2015 International Symposium on Advanced Electromechanical Motion Systems (ELECTROMOTION)* (pp. 1–10).
48. Chen, A., Nilssen, R., & Nysveen, A. (2010). Performance comparisons among radial-flux, multistage axial-flux, and three-phase transverse-flux PM machines for downhole applications. *IEEE Transactions on Industry Applications*, 46, 779–789. <https://doi.org/10.1109/TIA.2009.2039914>
49. Guo, YouGuang, Zhu, J. G., Watterson, P. A., & Wei, Wu. (2006). Development of a PM transverse flux motor with soft magnetic composite core. *IEEE Transactions on Energy Conversion*, 21, 426–434. <https://doi.org/10.1109/TEC.2005.860403>
50. Ahn, H., Jang, G., Chang, J., Chung, S., & Kang, D. (2008). Reduction of the torque ripple and magnetic force of a rotatory two-phase transverse flux machine using herringbone teeth. *IEEE Transactions on Magnetics*, 44, 4066–4069. <https://doi.org/10.1109/TMAG.2008.2001586>
51. Rodewald, W., Katter, M., & Vacuumschmelze. (2004). *Properties and applications of high performance magnets*.
52. Polinder, H., Mecrow, B. C., Jack, A. G., Dickinson, P. G., & Mueller, M. A. (2005). Conventional and TFPM linear generators for direct-drive wave energy conversion. *IEEE Transactions on Energy Conversion*, 20, 260–267. <https://doi.org/10.1109/TEC.2005.845522>
53. Oprea, CA, Martis, CS, Jurca, FN, Fodorean, D, Szabó, L, & Szabó, L (2011) Permanent magnet linear generator for renewable energy applications: Tubular vs. four-sided structures. In *2011 International conference on clean electrical power (ICCEP)* (pp. 588–592).
54. Mendes, R. G., Calado, M., & Mariano, S. (2014). *Identification of some tubular topologies of linear switched reluctance generator for direct drive applications in ocean wave energy conversion*.
55. Garcia-Tabares Rodriguez, L., Lafoz, M., Torres, J. J., Obradors, D., Blanco, M., Najera, J., Navarro, G., Garcia, F., & Sanchez, A. (2020). New type of linear switched reluctance generator for wave energy applications. *IEEE Transactions on Applied Superconductivity*, 1. <https://doi.org/10.1109/TASC.2020.2981900>
56. Lucas, J., & Pinilla, M. (2012). *Switched reluctance linear motor/generator*.
57. Blanco Aguado, M., Garcia Lorenzo, F. E., Garcia-Tabares Rodriguez, L., Lafoz Pastor, M., Obradors Campos, D., Torres Miranda, J. J., Jesus, M. O. C. D. T. M. J. (2019). *Switched reluctance machine*, 14.
58. Krishnan, R. (2001). *Switched reluctance motor drives: Modeling, simulation, analysis, design, and applications*. CRC Press.
59. Arghir, C., Jouini, T., & Dörfler, F. (2018). Grid-forming control for power converters based on matching of synchronous machines. *Automatica*, 95, 273–282. <https://doi.org/10.1016/j.automatica.2018.05.037>

60. Mohan, N., Undeland, T. M., & Robbins, W. P. (2003). *Power electronics: Converters, applications, and design*. Wiley.
61. Vukosavic, S., & Stefanovic, V. R. (1991). SRM inverter topologies: A comparative evaluation. *IEEE Transactions on Industry Applications*, 27, 1034–1047. <https://doi.org/10.1109/28.108453>
62. Bilgin, B., Jiang, J. W., & Emadi, A., *Switched reluctance motor drives: Fundamentals to applications*.
63. Barnes, M., & Pollock, C. (1998). Power electronic converters for switched reluctance drives. *IEEE Transactions on Power Electronics*, 13, 1100–1111. <https://doi.org/10.1109/63.728337>
64. Miller, T. J. E. (1989). *Brushless permanent-magnet and reluctance motor drives*. Clarendon Press.
65. Mikail, R., Husain, I., Sozer, Y., Islam, M. S., & Sebastian, T. (2013). Torque-ripple minimization of switched reluctance machines through current profiling. *IEEE Transactions on Industry Applications*, 49, 1258–1267. <https://doi.org/10.1109/TIA.2013.2252592>
66. Lin, F., & Yang, S. (2007). An approach to producing controlled radial force in a switched reluctance motor. *IEEE Transactions on Industrial Electronics*, 54, 2137–2146. <https://doi.org/10.1109/TIE.2007.895129>
67. Inderka, R. B., & De Doncker, R. W. A. A. (2003). High-dynamic direct average torque control for switched reluctance drives. *IEEE Transactions on Industry Applications*, 39, 1040–1045. <https://doi.org/10.1109/TIA.2003.814579>
68. Inderka, R. B., & De Doncker, R. W. A. A. (2003). DITC-direct instantaneous torque control of switched reluctance drives. *IEEE Transactions on Industry Applications*, 39, 1046–1051. <https://doi.org/10.1109/TIA.2003.814578>
69. Klein-Hessling, A., Hofmann, A., & De Doncker, R. W. (2017). Direct instantaneous torque and force control: A control approach for switched reluctance machines. *IET Electric Power Applications*, 11, 935–943. <https://doi.org/10.1049/iet-epa.2016.0515>
70. Wong, K. F., Cheng, K. W. E., & Ho, S. L. (2009). On-line instantaneous torque control of a switched reluctance motor based on co-energy control. *IET Electric Power Applications*, 3, 257–264. <https://doi.org/10.1049/iet-epa.2008.0124>
71. Vujičić, V. P. (2012). Minimization of torque ripple and copper losses in switched reluctance drive. *IEEE Transactions on Power Electronics*, 27, 388–399. <https://doi.org/10.1109/TPEL.2011.2158447>
72. Ilic'-Spong, M., Marino, R., Peresada, S., & Taylor, D. (1987). Feedback linearizing control of switched reluctance motors. *IEEE Transaction on Automatic Control*, 32, 371–379. <https://doi.org/10.1109/TAC.1987.1104616>
73. Sahoo, N. C., Xu, J. X., & Panda, S. K. (2001). Low torque ripple control of switched reluctance motors using iterative learning. *IEEE Transactions on Energy Conversion*, 16, 318–326. <https://doi.org/10.1109/60.969470>
74. Mir, S., Elbuluk, M. E., & Husain, I. (1999). Torque-ripple minimization in switched reluctance motors using adaptive fuzzy control. *IEEE Transactions on Industry Applications*, 35, 461–468. <https://doi.org/10.1109/28.753642>
75. Blanco, M., Navarro, G., & Lafoz, M. (2009). Control of power electronics driving a switched reluctance linear generator in wave energy applications. In *13th European Conference on Power Electronics and Applications, 2009. EPE '09* (pp 1–9). IEEE.
76. Hull, J. R., Wilson, M. N., Bottura, L., Rossi, L., Green, M. A., Iwasa, Y., Hahn, S., Duchateau, J.-L., & Kalsi, S. S. (2015). Superconducting magnets. *Applied superconductivity* (pp. 403–602). Weinheim, Germany: Wiley-VCH Verlag GmbH & Co. KGaA.
77. Iwasa, Y. (2009). *Case studies in superconducting magnets: Design and operational issues* (2nd ed.). US: Springer.
78. Dolan, T. J. (2013). Cryogenic systems. In *Lecture Notes in Energy* (pp 491–511). Springer.
79. Terao, Y., Sekino, M., & Ohsaki, H. (2010). Design study of linear synchronous motors using superconducting coils and bulks. In *The 2010 international power electronics conference—ECCE ASIA* (pp. 1760–1765).

80. Jin, J. X., Zheng, L. H., Guo, Y. G., & Zhu, J. G. (2011). Performance characteristics of an HTS linear synchronous motor with HTS bulk magnet secondary. *IEEE Transactions on Industry Applications*, 47, 2469–2477. <https://doi.org/10.1109/TIA.2011.2168934>
81. Hodgins, N., Keysan, O., McDonald, A. S., & Mueller, M. A. (2012). Design and testing of a linear generator for wave-energy applications. *IEEE Transactions on Industrial Electronics*, 59, 2094–2103. <https://doi.org/10.1109/TIE.2011.2141103>
82. Keysan, O., & Mueller, M. A. (2012). A linear superconducting generator for wave energy converters. In *6th IET International conference on power electronics, machines and drives (PEMD 2012)* (pp. 1–6).
83. García-Tabarés, L., Munilla, J., López de Toledo, C., García, F., Sarmiento, G., & Sanz, S. (2020). *Máquina Eléctrica Lineal Superconductora de Movimiento Alternativo*.
84. Lucas, T. J., & Pinilla, M. M. (2006). *Switched reluctance linear motor/generator*.

Open Access This chapter is licensed under the terms of the Creative Commons Attribution 4.0 International License (<http://creativecommons.org/licenses/by/4.0/>), which permits use, sharing, adaptation, distribution and reproduction in any medium or format, as long as you give appropriate credit to the original author(s) and the source, provide a link to the Creative Commons licence and indicate if changes were made.

The images or other third party material in this chapter are included in the chapter's Creative Commons licence, unless indicated otherwise in a credit line to the material. If material is not included in the chapter's Creative Commons licence and your intended use is not permitted by statutory regulation or exceeds the permitted use, you will need to obtain permission directly from the copyright holder.

